Univerza
v Ljubljani

Naravoslovnotehniška
fakulteta

Oddelek za geologijo

Aškerčeva 12
1000 Ljubljana
telefon: 01 470 46 32
faks: 01 470 45 60
p.p.312
e-mail:
spela.turic@.ntf.uni-lj.si

datum: Oktober, 2014

CONTRACTING AUTHORITY: GEOLOŠKI ZAVOD SLOVENIJE
Dimičeva ulica 14
1000 Ljubljana

PETROLOGIC-MICROTECTONIC ANALYSES OF CLEAVED LIMESTONE ON THE KRAS AREA

Annex 2.1

Contract: No. 1130-72/2014

Author of report:
Assoc. prof.dr. Andrej Šmuc

Head of the Geology department:
Assoc. prof dr Mihael Brenčič

CONTENT

I. INTRODUCTION

The Classical Karst represents a well-defined geographical unit with unique geological, geomorphological and hydrogeological and also architectural and cultural characteristics. The word kras (or karst in English literature) origins from the ancient word for stone: ka(r)a/gs(r)s“ that gave the origin to the ancient name for the region in Roman times: *Carusaud, Karusad, Carsus.* This word slowly changed into Kras (Slovene), Karst (German), and Carso (Italian). Word KRAS in Slovenian has different meanings: on one hand it represents a specific geographical area, while on the other it is also name of a specific type of landform. As a geographical name the Kras is a limestone plateau, located in northernmost part of the Adriatic Sea, above the Trieste bay. The 45^0 45' parallel runs through the middle of the Kars and 14^0 00' meridian east is crossing it east of the main city on Karst: Divača. Although the Kras plateau is not very high (from 200 to 500 m a.s.l.) it is well defined. To the SW it rises over Trieste bay, to the N it is surrounded by alluvial Soča plain and Vipava valley, while the SE border is well defined by Brkini Hills and the Reka river Valley. As a geomorphological term the word kras represents a type of terrain with a distinctive assemblage of landforms and hydrology arising from a combination of high rock solubility and well developed secondary porosity, where special superficial and underground features developed and where underground water drainage is in control (figure I-1).

The Karst region is one of the most interesting areas containing reserves of natural stones in Slovenia because the limestone has always played a crucial role in the cultural heritage, landscape and economy of the Italian and Slovenian Karst area. The reason for this can mainly be sought in the fact that the majority of the Karst area is composed of Cretaceous to Paleogene shallow-to deeper-water limestone reaching more than 2000m of thickness. These limestones, divided into various formations, are an important economic and architectural resource for the Classical Karst region, as they provide high-quality natural stones. Since long ago these stones have been appreciated as a result of their sound geomechanical properties and versatility. Thus the Karst region has been associated with the quarrying and manufacturing of stone over two thousand years, since Roman period. Large number of quarries of different types of limestone can be found and documented (figure I-2); however many of them are not active nowadays.

Figure I-1: Škocjan Caves National Park

Figure I-2: Active quarry of the Lipica unito and Lipica fiorito building and ornamental stones.

Almost all of the rock types found in Kras area were used for this or that purpose. The thicker bedded limestones were used for basic structure of the typical Kras house and also for other architecture elements, such as the shelves, corner-stones, window frames, doorposts, stairs and pavements (inside termed *škrle*, outside *šeliž*). However of special interest are so called platy limestones: these were used mainly for tilling the roofs, walls and fireplaces. The platy limestones occurs various geological formations in Classical Karst in seemingly very similar forms. They are known under the names of Komen and Tomaj limestones and even Komen fish shales (mainly due to the frequent finds of fossil fish). The RoofOfRock Project (funded under the Adriatic IPA CBC Programme 2007 – 2013) aims to propose a use of environmentally compatible platy limestone, to encourage its promotion and protection and to develop useful guidelines for its sustainable use as a natural and cultural heritage.

However within the primary research of the RoofOfRoock project it was noted that not all of the ''platy'' limestones belong to the Komen and Tomaj variation of the thin-bedded to laminated limestones. Moreover in more than a 50% the obtained rock slabs were not cut from the laminated limestone but actually from light-gray, massive or at least thick-bedded limestones belonging to other formations (for example Repen and Lipica Formations) (figure I-3). The possibility to obtain relatively large and thin slabs of limestone from this type of limestone is connected with the tectonic deformation caused by dextral strike-slip faulting that affected the area in Neogene. The limestones were fractured in dense and aligned fractures or joint systems. In these places the limestone slabs were easily obtained using picks and levers, or, more rarely chisels. In the past in both in Italy and Slovenia, several outcrops, termed *jave* by locals and located closest to the villages, were used as sources for platy limestones. To distinguish them from the sedimentary platy limestones, we are using the working term **''fractured limestone**''.

Figure I-3: active Griža (Tavčar) quarry where cleaved limestone is extracted.

AIMS OF RESEARCH

The ''classical'' platy limestone refers to the Upper Cretaceous limestones where foliation is defined with sedimentary structures of lamination and thin-bedding of the rock. These textures range in thickness from around 1mm to few centimeters. These bedding planes of course represent the planes of weakness and allowed the local builders in the Kars region to easily obtain a relatively thin and large limestone slabs that were mainly used for tilling. This type of the tilling also signifficaly marked the **typical** Karstic architecture and thus represents an important aspect for cultural and natural heritage and preservation. Unfortunately the desired foliation stopped to be desired after it was built into the roof. Namely, the cleaving of the slab did not at that time but continued even after the slab was excavated and built into the roofs. Not only the lamination but also the preferred bedding-parallel orientation of the elongated grains and in some cases also large quantity of organic matter caused additional cleaving of the slabs after their use.

During initial research it was noted that not all of limestone slabs were obtained from the thin-bedded and laminated limestones. In places also massive and thick-bedded parts of the Cretaceous formations were used. Here the foliation is not defined by sedimentary structures but is a tectonic feature and related to fissure system) that divided rocks into thin slabs. In order to separate this ''non-classical'' platy slabs we used a name **cleaved** limestone to denote their tectonic origin. Additionally it was also noted that these slabs are much more durable and resistible compared to the ''classical'' platy limestone slabs.

The aims of this present research was to define the main petrographic, sedimentologic and microtectonic aspects of the so called **cleaved** limestone in order to get a better insight into the mechanisms of their formation and to perhaps give the end-users a guidelines into finding new and also old and forgotten quarries of this high-quality slabs.

II. GEOLOGICAL SETTING

II.A. STRUCTURAL SETTING

In a broader sense the Kras, or the Trieste-Komen plateau belong to the northern part the Adriatic micro continent that was in the Mesozoic bordered by Alpine Tethys, Meliata and Vardar oceans. In regional scale the area belongs to the northwestern most part of the External Dinarids and forms an anticlinorium in the NW-SE direction (figure II A-1). In narrower structural sense the Karst belongs to the Komen thrust sheet that was overthrusted on the Adriatic foreland towards SW in Oligocene-Miocene. The Komen thrust sheet is overthrusted by a Snežnik and Hrušica napes (Placer 1999, 2008). According to the Buser (1973), Jurkovšek et al. (1996) and Poljak (2007) the Karst region belongs to the Trieste-Komen anticlinorium that passes north and northeast to the Gorica and Vipava synclinorium and to the southwest into Rijeka synclinorium.

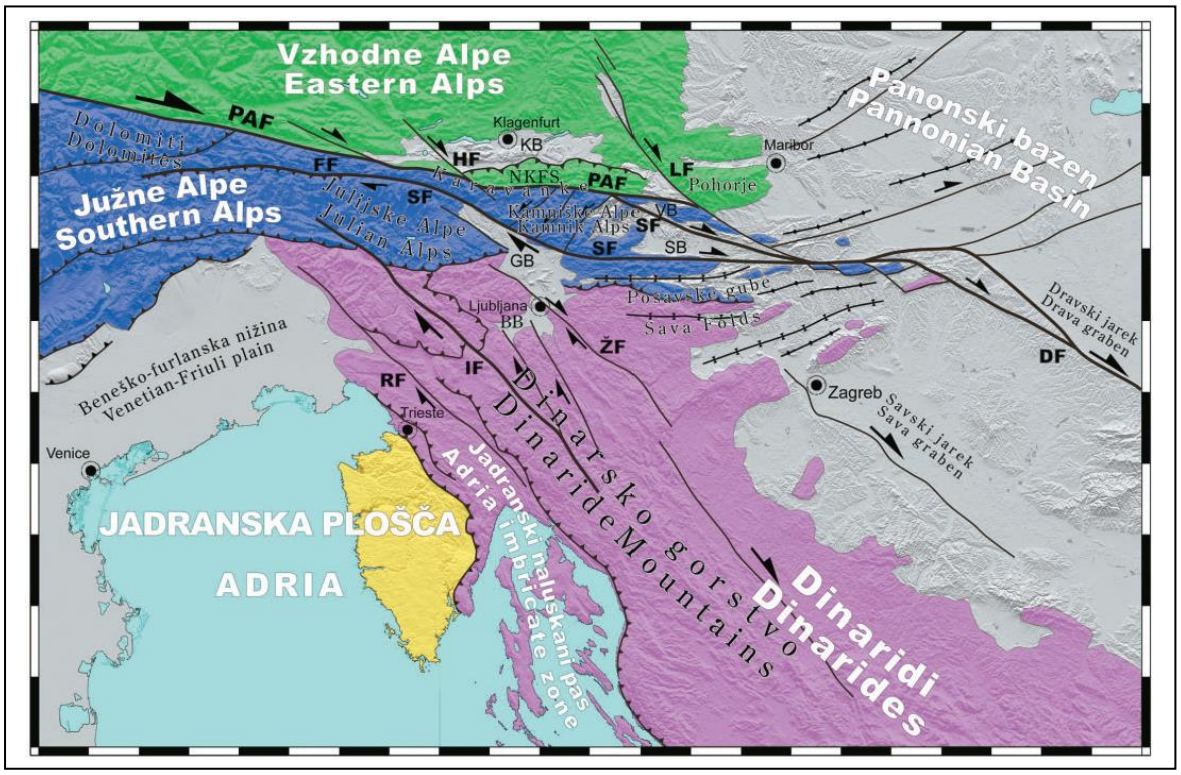

Figure IIA -1. Simplified tectonic map of the north-eastern corner of the Adria-Europe collision zone with principal geographic features (Vrabec et al. 2009).

At the transition from the Miocene to the **Pliocene**, the final closure of the oceanic embayment in the Carpathians stopped the eastward extrusion of the Eastern Alps, causing a major re-organization of the tectonic regime in the region (Vrabec & Fodor, 2006). Paleomagnetic data suggest that the Adriatic microplate started rotating in the CCW sense at about the same time. These resulted in dextral transpression. Southern and southwestern Slovenia was and is extensively faulted by NWSE- trending dextral faults, which form conspicuous topographic lineaments, particularly in karstic areas. Since the faults are parallel to the strike of Dinaric folds and thrusts, they are classically called Dinaric faults, but no structural connection with Dinaric thrusting is known. These faults cut and displace both Dinaric and South-Alpine fold-and thrust structures. The average displacement is in the range of several kilometers and seems to become progressively smaller on the faults lying toward the southwest. The largest dextral offset known is about 12 km, and was inferred for Idrija fault on the base of displaced geological and geomorphological markers. Fault-slip data and map relationships indicate that many of the faults, including Idrija fault, formed as dip-slip normal faults and were only later dextrally reactivated. On the grounds of recent and historic seismicity it is believed that at least some of the Dinaric faults are active today (e.g., Poljak et al., 2000).

II.B. PALAEOGEOGRAPHICAL SETTING

In the Mesozoic the research area belonged to the south Tethyan passive continental margin that was experienced extension related to the rifting. The region of the Karst belonged to Adriatic-Dinaric Carbonate Platform, a long lasting carbonate platform in the Mediterranean. There is more than 2000m thick sequence of predominantly shallow-marine carbonate rocks outcropping in the Karst region today (Jurkovšek et al. 1996, 2013). This sequence has over Cretaceous to Eocene sedimented on the northern part of the Adriatic-Dinaric Carbonate Platform (Gušić & Jelaska 1993, Jelaska et al. 1995, Šribar et al. 1995, Steuber et al. 2005, Placer 2008) or Adriatic Carbonate Platform (Vlahović et al. 2002, 2005, Dragičević & Velić 2002).

The investigated sections are located near the Divača fault in the central part of the Kars area (figure IIB -1)

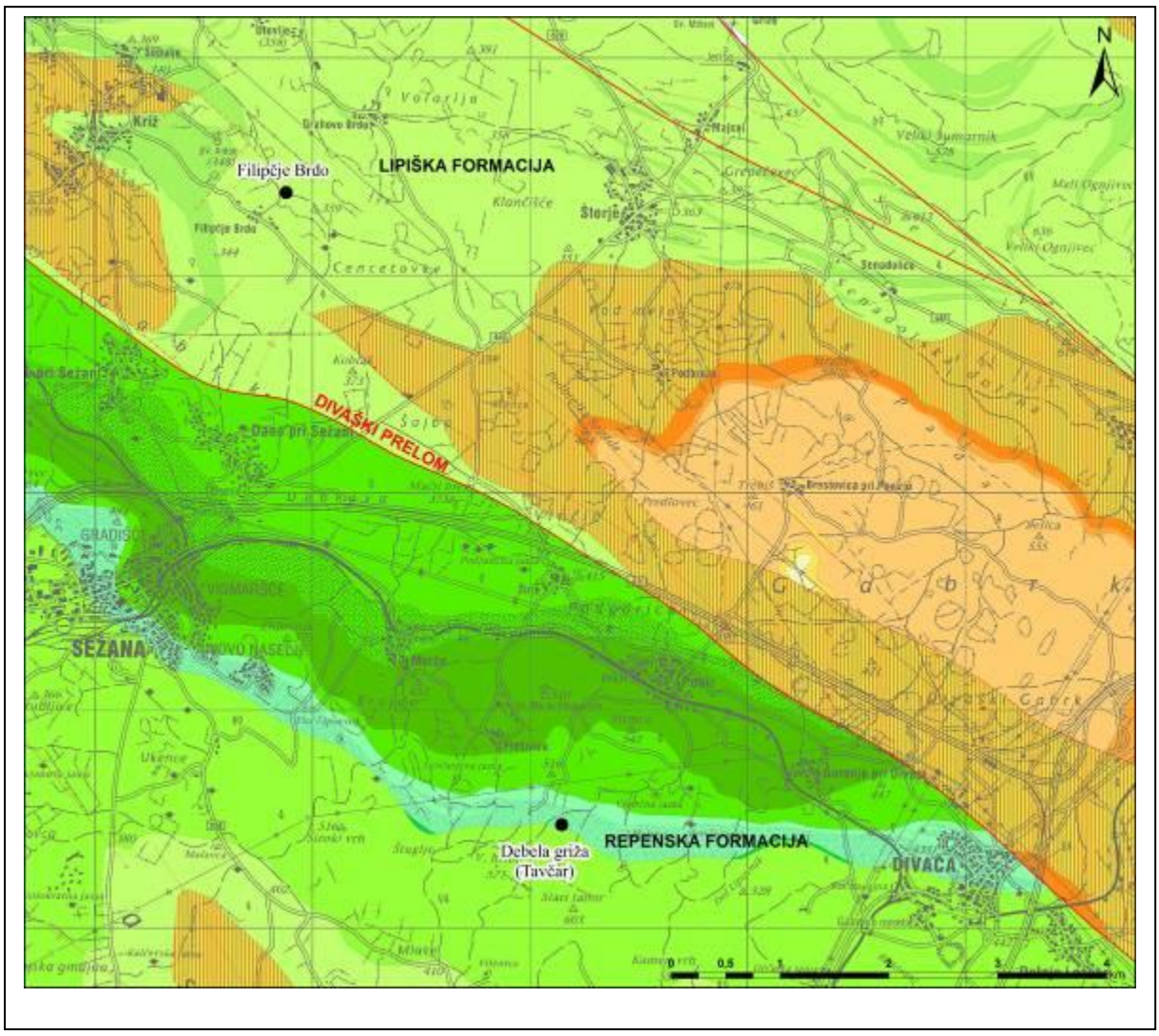

Figure IIB -1: Sector of the geological map of the Karst area, with marked investigated locations. (Modified after Jurkovšek et al. 2013).

III. MATERIALS AND METHODS

III.A. FIELD WORK

A detailed field work was carried in 2014. Among the almost 20 active and abandoned quarries two localities where **fractured** limestone slabs were excavated.

Debela Griža (Tavčar quarry) is active quarry where Repen type of limestone is excavated. In the eastern part of the quarry the small surface sub-quarries (5x5m) are still visible, from where the local builders were excavating slabs of fractured limestone. Today the area is completely covered by vegetation, however outcrops of new quarry enable detailed work (photo IIIA -1).

Photo IIIA -1: Debela Griža (Tavčar quarry). At the back wall of the quarry, the fractured limestone is clearly visible.

Filipčje Brdo is an outcrop located northward from the village of the Filipčje Brdo. Here the outcrop of old and abandoned surface quarry is 100 x 100m large. Here the local builders were excavating slabs of the Lipica formation limestone. These slabs were used for tilling the roofs of the Filipčje Brdo and Križ villages. On the location the signs of renewed: fresh excavating activity is visible (photo IIIA -2).

Photo IIIA -2: Filipčje Brdo.The renew activity of slab retrievement is clearly visible.

IIII.B. PETROGRAPHIC MICROSCOPY

From the outcrops 7 samples were collected and 10 thin sections were prepared for microfacies and microtectonic investigations (rock samples, thin sections, and SEM samples are stored at the Geology Department, NTF, University of Ljubljana). Thin sections were investigated under the Carl Zeiss optical microscope. The samples were photographed with digital camera AxioVision LE (AxioVs40 V4.7.1.0). The classification of the limestones is based on the Folk (1959) with improvement (1962) and Dunham (1962) with improvement of Embry & Klovana (1972). The microtectonic features were described according to the modified morphological classification of foliations after Powell (1979) and Borradaile et al. (1982).

III.C. SCANNING ELECTRON MICROSCOPE (SEM)

Characteristics of surfaces along which platy and, cleaved limestone split were investigated in a JEOL JSM 6490LV scanning electron microscope (SEM), using high vacuum. SEM is coupled with an Oxford INCA energy dispersive spectroscopy (EDS) system, comprising Oxford INCA PentaFETx3 Si(Li) detector and INCA Energy 350 processing software, at 20 kV accelerating voltage, spot size 50, and 10 mm working distance. The sample surfaces were examined in backscattered electron (BSE) and secondary electron (SE) modes. Due to strong charging of samples, they were coated by gold and carbon. Nevertheless, the BSE images are useless, while x-ray compositional diagrams show weakened peaks on the left side of the presented diagrams.

IV. RESULTS

IV.A. FIELD WORK

LOCATION 1

Name: Griža (Tavčar) (see figure IIB-1, and IVA 1-6)

Samples code: DG

GPS coordinates:

x: 5061072; y: 5416146 (GK)

LAT: 45° 41' 19.67''; LON: 13° 55' 07.06'' (WGS84)

Geological formation: Repen formation

Type of limestone: Repen

Azimuth and inclination of beds: 220/25

Azimuth and inclination of main fissure system : 100/90 (+/- 10°);
The distance between larger faults and joints ranges from 2-5m. Cleavage or fissure systems are parallel with these faults.
In the cut walls of the quarry it is noted that the average distance between the individual fissures in the fissure system is around 5cm. These fissures penetrate at least 5m deep into the rock.
In the upper 2m these fissures are strongly carstified.

Lithology: light gray, thick-bedded, coarse-grained biomicritic limestone (biocalcrudite)

List of samples:

- DG -1 lower-western part of the quarry
- DG_Z – 1 lower-western part of the quarry, partly karstified fissures
- DG_Z – 2 lower western part of the quarry, partly karstified fissures
- GRIŽA upper-eastern part of the quarry

Foto IVA1-1: Fractured limestone of the Debela Griža Quarry

Foto IVA1-2: Fractured limestone of the Debela Griža Quarry.

Foto IVA1-3: Fractured limestone of the Debela Griža Quarry

Foto IVA1-4 Fractured limestone of the Debela Griža Quarry

Foto IVA1-5: Fractured limestone of the Debela Griža Quarry

Foto IVA1-6 Fractured limestone of the Debela Griža Quarry

LOCATION 2

name: Filipčje Brdo (see figure IIB-1, and IVA2 1-6)

Sample code: FB

GPS coordinates:

x: 5066589; y: 5414069 (GK)

LAT: 45° 44' 17.43''; LON: 13° 53' 27.56'' (WGS84)

Geological formation: Lipica Formation

Limestone type: Lipica unito

Azimuth and inclination of beds: On the exact spot of location it was impossible to measure the bedding. Approximately 200m west from the location the azimuth and inclination of beds is 260/20.

Azimuth and inclination of beds of small fissure system: 260/80

Lithology: bedded, light gray, fine-grained biomicritic limestone (biocalcarenite)

List of samples

- FB – 1
- FB – 2
- FB – 3
- FB - 4

Foto IVB2-1: Fractured limestone of the Filipčje Brdo

Foto IVB2-2: Fractured limestone of the Filipčje Brdo

Foto IVB2-3: Fractured limestone of the Filipčje Brdo

Foto IVB2-4: Fractured limestone of the Filipčje Brdo

Foto IVB2-5: Fractured limestone of the Filipčje Brdo

Foto IVB6-6: Fractured limestone of the Filipčje Brdo

IV.B. HOST ROCK MICROFACIES

Location Grižе: SAMPLE DG-1

Texture

Sample exhibit non-homogeneous texture visible as approximately bedding parallel alternation of densely- packed grainstone/packstone to rudstone and loosely-packed packstone. In densely-packed packstone to rudstone the grain/matrix ratio is more than 60/40 (photo IVB1-1), while in the loosely-packed packstone the ratio is 40/60 (photo IVB1-2). In the densely-packed parts the size of the grains range from 100 µm to few centimeters, on average the grains are 0,5 to 1cm large. In loosely-packed packstone the grains are smaller ranging from 40 to 200 µm. In the densely-packed parts the grains are poorly sorted, at places with preserved original shape, while more common angular to sub-rounded. The grains mainly exhibit point, line and concavo-convex contacts. In loosely-packed packstone the grains are well sorted, sub-rounded, and exhibit mainly point contacts.

In both variations the matrix is micrite that is partly recrystallized into microsparite.

The sample exhibits no intergranular, modlic shelter and intraparticle porosity. On the other hand the samples exhibit a system of microcracks (discussed in detail in chapter IV-C).

Foto IVB1-1: densely-packed packstone with mainly recrystalised bioclasts (rudists?).

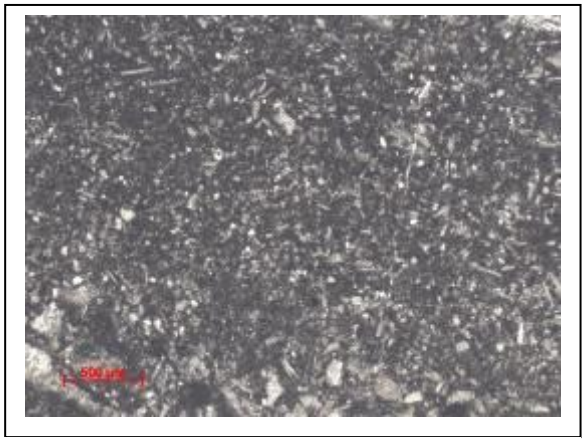

Foto IVB1-2: loosely-packed packstone with small sparitic bioclasts.

Composition

The grains in the sample constitute solely of alochems more exactly bioclasts. Most common are fragments of bivalves (inoceramid and rudist shells?) that represent 90% of grains. They range

from quite fragmented to partly fragmented shell, while complete shells are rare. They are in size ranges from 100 µm to few centimeters, on average form 0,5 to 1cm. The fragments are poorly sorted, usually the internal structure is not preserved due to the recrystallization. They exhibit normal prismatic microstructure composed of the individual calcite prisms that act as a single crystals (photo IVB1-3, photo IVB1-4). Only in rare cases the internal structure is preserved (photo IVB1-5, photo IVB1-6).

Other 10% grains are represented by a small, rounded grains belonging to calcispheres (more common in the loosely- packed packstone) (photo IVB1-7), fragments of foraminifers (photo IVB1-8), echinoderm fragments (photo IVB1-9), and intraclasts.

Foto IVB1-3: The bioclasts with prismatic microstructure (parallel Nichols)

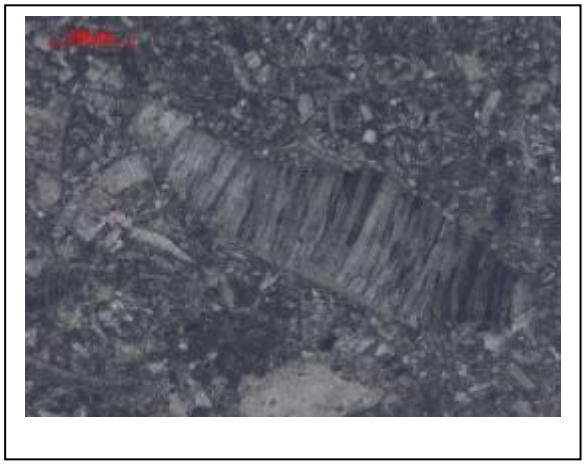

Foto IVB1-4 The bioclasts with prismatic microstructure (crossed Nichols)

Foto IVB1-5: densely packed packstoone with rudist? shells.

Foto IVB1-6: densely packed packstoone with rudist? shells.

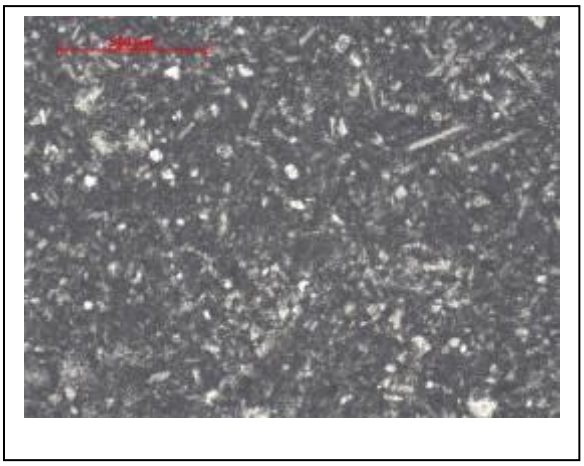

Foto IVB1-7: loosely-packed packstone with small sparitic bioclasts: calcispheres

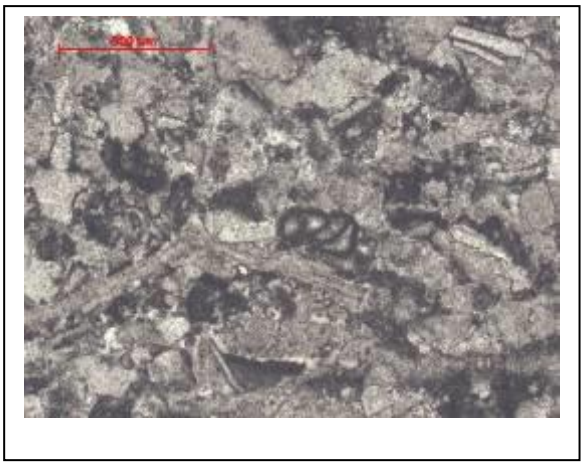

Foto IVB1-8: densely-packed packstone with visible foraminfera fragment.

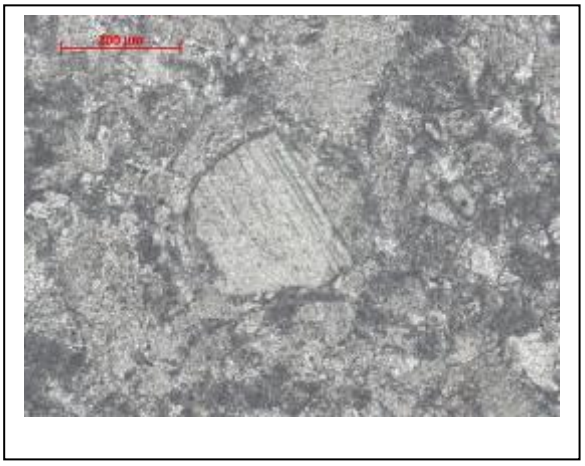

Foto IVB1-9: densely-packed packstone with visible echinoderm fragment.

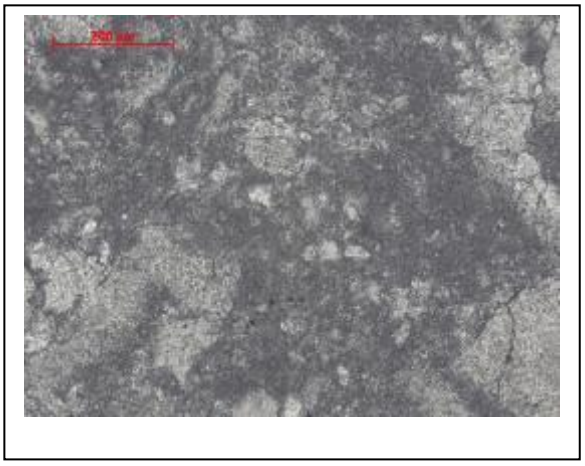

Foto IVB1-10: Partly recrystallised micritic matrix

Matrix

The matrix of the sample is composed of the micrite that is partly recrystallized into microsparite (photo IVB-10).

Location Griže: SAMPLE DG_Z-1

Texture

Sample exhibit non-homogeneous texture of rudstone and packstone that are alternating within irregular fields (photo IVB2-1 and IVB2-2). In rudstone the grain/matrix ratio is approximately 60/40 (photo IVB2-1), while in the packstone the ratio is 50/50 (photo IVB2-2). In the rudstone the size of the grains range from 100 µm to few centimeters, on average the grains are 0,5 to 1cm large. In the packstone the grains are smaller ranging from 100 to 400 µm reaching average around 200 µm. In the rudstone the grains are poorly sorted, at places with preserved original shape, while more common angular to sub-rounded. The grains mainly exhibit point and line contacts, while and concavo-convex contacts appear rarely. In packstone the grains are well sorted, sub-rounded, and exhibit mainly point contacts.

In both variations the matrix is micrite that is partly recrystallized into microsparite. In some of the larger clasts the matrix is also represented by a larger sparite

The sample exhibits no intergranular, modlic shelter and intraparticle porosity. On the other hand the samples exhibit a system of microcracks (discussed in detail in chapter IV-C).

Foto IVB2-1: rudstone with fragments of bivalves, gastropods, brachiopods other bioclasts.

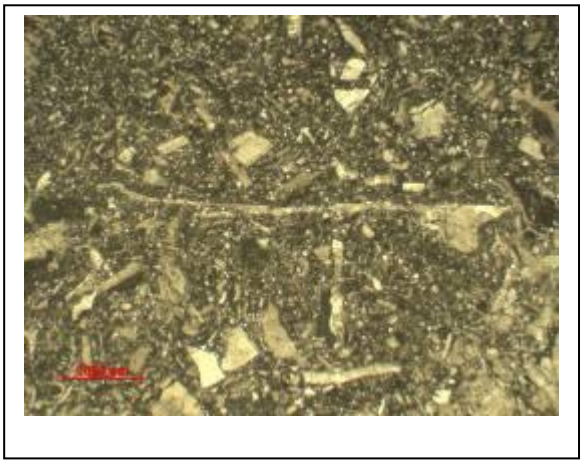

Foto IVB2-2: loosely-packed packstone with small sparitic bioclasts.

Composition

The grains in the sample constitutes solely of bioclasts. Most common are fragments of bivalves (inoceramid and rudist shells?) that represent 90% of grains. They range from quite fragmented to partly fragmented shells, while complete shells are rare (photo IVB2-3). They are in size ranges from 100 µm to few centimeters, on average form 0,5 to 1cm. The fragments are poorly sorted, usually the internal structure is not preserved due to the recrystallization. They exhibit

normal prismatic microstructure composed of the individual calcite prisms that act as a single crystals- similar as a sample DG-1 (photo IVB2-4). Common is also lamellar composition of the shells that could represents preserved original structure of the shell (photo IVB2-5). At places the lamellar structure of the shell is visible only as a ghost within recrystallized calcite prisms (IVB2-6).
Other 10% grains are represented by a small, rounded grains belonging to calcispheres (more common in the packstone) (photo IVB2-7), intraclasts of rounded to sub-rounded mudstones (photo IVB2-8) and also clasts composed of fine-grained sparite (photo IVB2-9).

Foto IVB2-3: The bioclasts of bivalvs with preserved original shape

Foto IVB2-4 The bioclasts with prismatic microstructure (crossed Nichols)

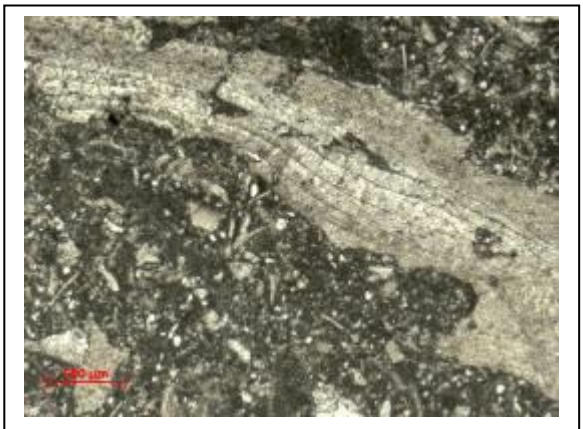

Foto IVB2-5: the bioclasts with prserved lammelar structure of the shell.

Foto IVB2-6:packstone with rudist? Shell with visible 'ghost' lamelars structure.

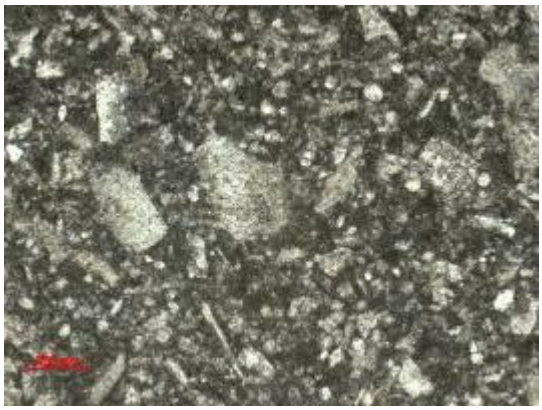

Foto IVB2-7: packstone with calcispheres and other bioclasts.

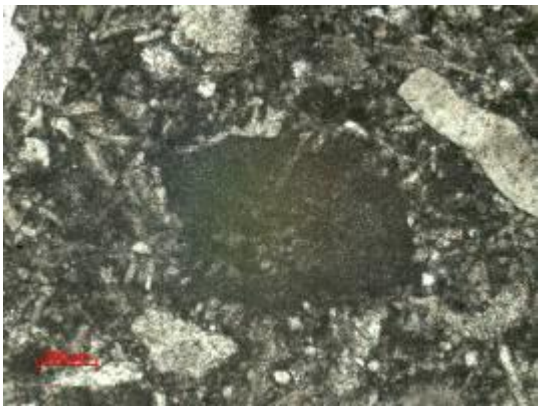

Foto IVB2-6:packstone mudstone intraclasts structure.

Matrix

The matrix of the sample is composed of the micrite that is partly recrystallized into microsparite (photo IVB-10). Rarely also mosaic sparite cements are present. They usually occur within larger hollow clasts and completely fill them (photo IVB-11).

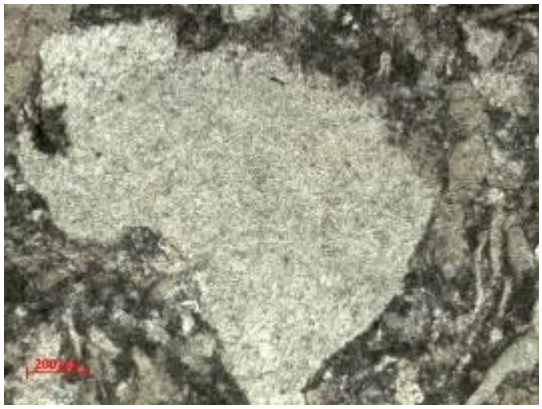

Foto IVB2-9: grainstone with sparitic clast.

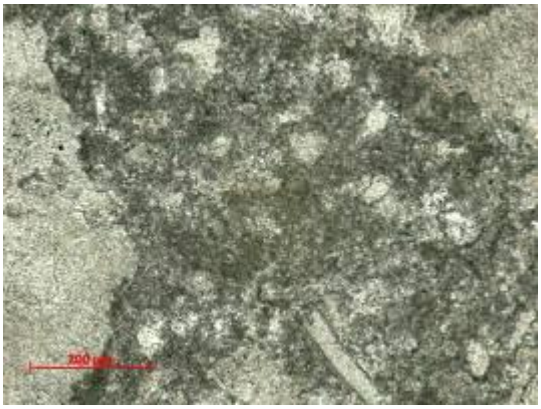

Foto IVB2-10: Partly recrystallised micritic matrix.

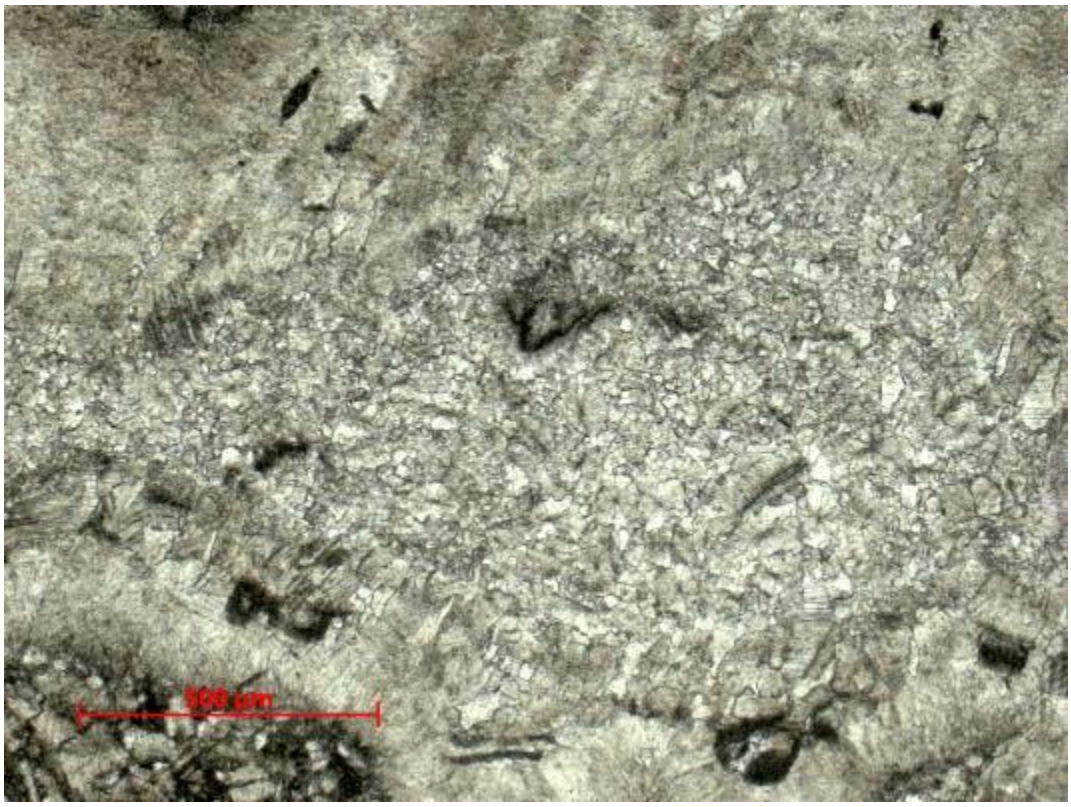

Foto IVB2-11: Mosaic sparite cement filling the bivalve shell.

Location Grižе: SAMPLE DG_Z-2

Texture

Sample exhibit relatively homogeneous texture with uniform fine-grained packstone (photo IVB3-1). Only rarely the larger bioclasts appear (photo IVB3-2). The grain/matrix ratio is around 45/55 (photo IVB3-1). The size of the grains range from 100 µm to few centimeters, on average the grains are 0,4 to 1cm large. The grains are poorly to moderately sorted, and angular to sub-rounded, while at places grains with preserved original shape occur. The grains mainly exhibit point and line contacts, while concavo-convex contacts are rare.

The matrix is micrite that is partly recrystallized into microsparite.

The sample exhibits no intergranular, modlic shelter and intraparticle porosity. On the other hand the samples exhibit a system of microcracks (discussed in detail in chapter IV-C).

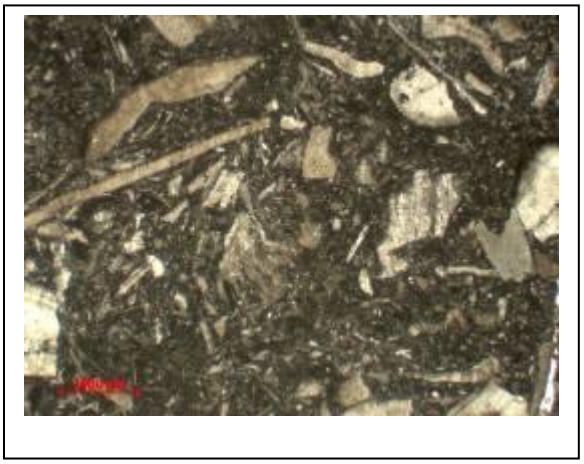

Foto IVB3-1: fine-graiend packstone with mainly recrystalised bioclasts of bivalves (inoceramids and rudists?).

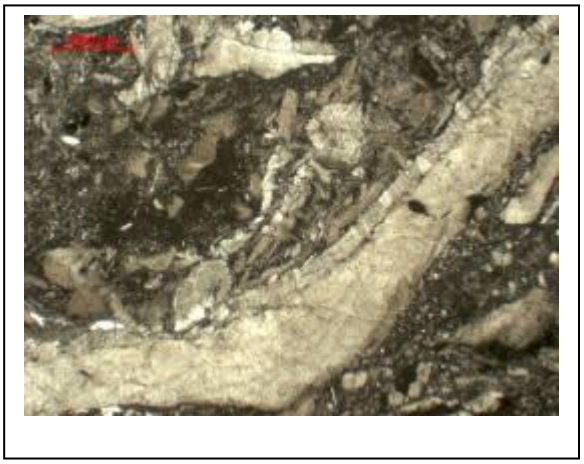

Foto IVB3-2: larger bioclast within fine-grained pacskstone.

Composition

The grains in the sample constitutes of bioclastic debris. Most common are fragments of bivalves (inoceramid and rudist shells?) that represent 90% of grains. They range from quite fragmented to partly fragmented shells, while complete shells are rare. They are in size ranges from 100 µm to few centimeters, on average form 0,4 to 1cm. The fragments are poorly sorted, usually the internal structure is not preserved due to the recrystallization. They usually exhibit normal prismatic microstructure composed of the individual calcite prisms that act as a single crystals. Common is also lamellar composition of the shells that could represents preserved original structure

of the shell (photo IVB2-3). At places the lamellar structure of the shell is visible only as a ghost within recrystallized calcite prisms (photo IVB2-4). However also clasts that are completely recrystallized into fine-grained sparite are present (photo IVB2-5).

Other 10% grains are represented by a small, rounded grains belonging to calcispheres (photo IVB3-6) that range in size from 40 µm -80 µm and are well sorted, and echinoderms. Echinoderms are quite fragmented and up to 0,5cm large.

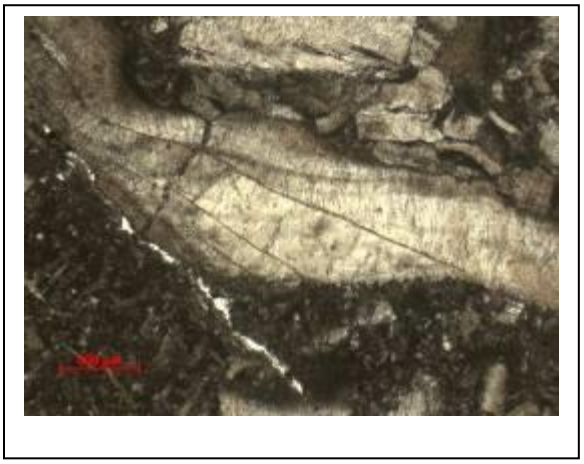

Foto IVB3-3: The bioclasts with prismatic microstructure.

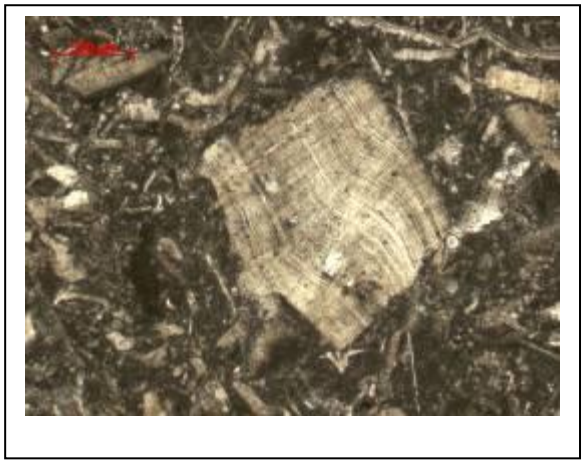

Foto IVB3-4: packstone with rudist? Shell with visible 'ghost' lamelars structure.

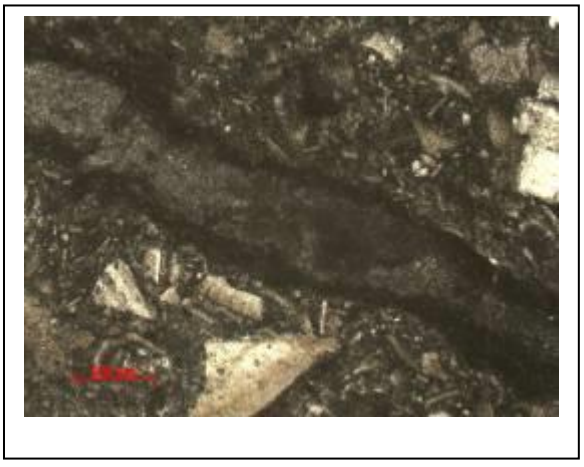

Foto IVB3-5: packstone with completely recrystalised shell fragment..

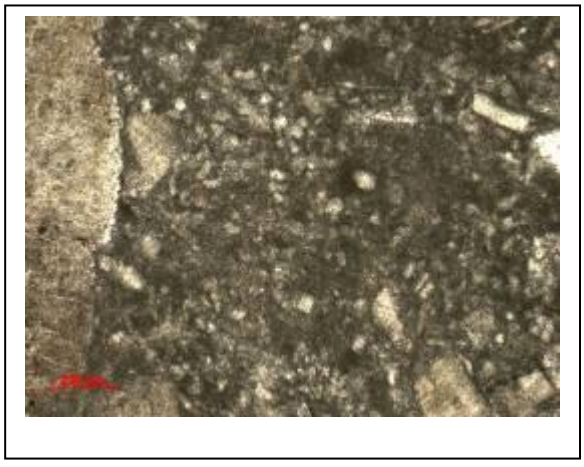

Foto IVB3-6: calcispheres within packstoone.

Matrix

The matrix of the sample is composed of the micrite that is partly recrystallized into microsparite.

Location Griže: SAMPLE Griža

Texture

Sample exhibit homogeneous texture of densely- packed packstone to rudstone. In comparison with previous samples the grain/matrix ratio can reach almost 80/20 (photo IVB4-1 and IV4-2). The size of the grains range from 100 µm up to 5 centimeters, on average the grains are 0,2mm to 10mm large. Grains are poorly sorted and two size populations are visible. In larger the grains range from 1mm up, while in finer grains are usually smaller than 0,7mm. Larger and elongated grains are clearly oriented approximately parallel to the bedding (photo IVB4-3). Grains are with preserved original shape are rare while more common angular to sub-rounded. The grains mainly exhibit line and concavo-convex contacts while the point contacts are rare.

The matrix is micrite that is partly recrystallized into microsparite.

The sample exhibits no intergranular, modlic shelter and intraparticle porosity. On the other hand the samples exhibit a system of microcracks and also pores that represents enlarged parts of the crack (photo IVB4-4) discussed in detail in chapter IV-C).

Foto IVB4-1: densely-packed packstone/rudstone.

Foto IVB4-2: densely-packed packstone/rudstone.

Composition

The grains in the sample constitutes mainly of bioclasts. Most common are fragments of bivalves (inoceramid and rudist shells?) that represent 90% of grains. They range from quite fragmented to partly fragmented shells, while complete shells are rare. They are in size ranges from 100 µm to 5 centimeters, on average form 0,5 to 1cm. The fragments are poorly sorted, usually the internal structure is not preserved due to the recrystallization. Numerous clasts are exhibiting highly corroded and/or bored surface (photo IVB4-5, photo IVB4-6). Almost all the clasts exhibit normal

prismatic microstructure with individual calcite prisms. Only in rare cases the internal structure is preserved.

Other 10% grains are represented by a small, rounded intraclasts of the mudstones (photo IVB4-7), calcispheres, elongated small sparitic fragments and also some echinoderms (photo IVB4-8).

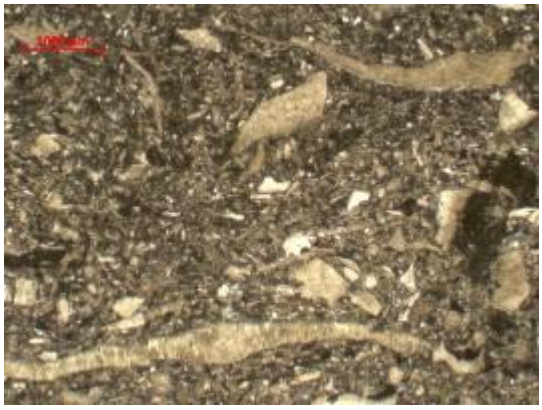

Foto IVB4-3: The bedding-parallel orientation of the larger bioclasts.

Foto IVB4-4 Packsotone with bioclasts and visible pore in the middle of the photo.

Foto IVB4-5: packstoone/rudstone with coroded inoceramus or rudist shells.

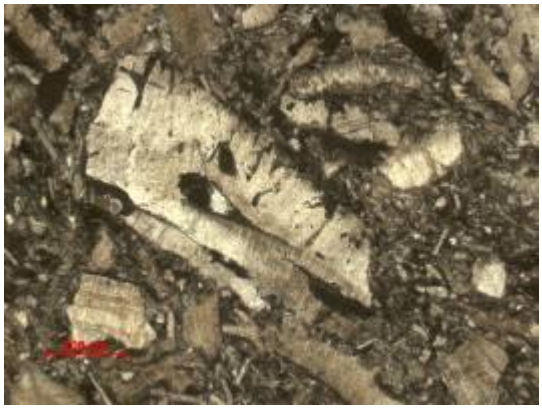

Foto IVB4-6: densely packed packstoone with rudist? shells.

Matrix

The matrix of the sample is composed of the micrite that is partly recrystallized into microsparite (photo IVB4-9).

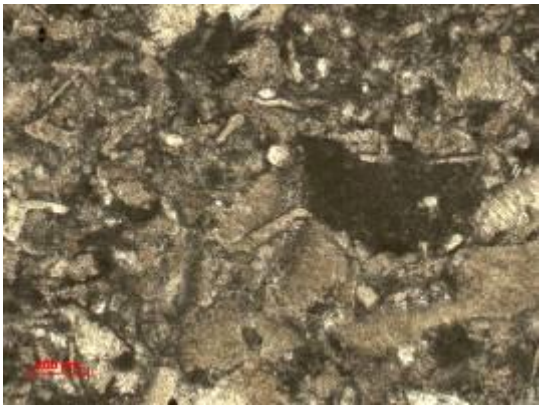

Foto IVB4-7: packstone- rudstone vith small intraclast of mudstone

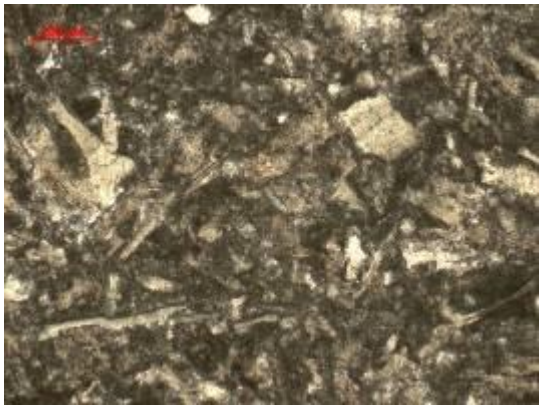

Foto IVB4-8: pakckstoe-rudstone with calcispheres, elongated sparitic grains and echinoderms.

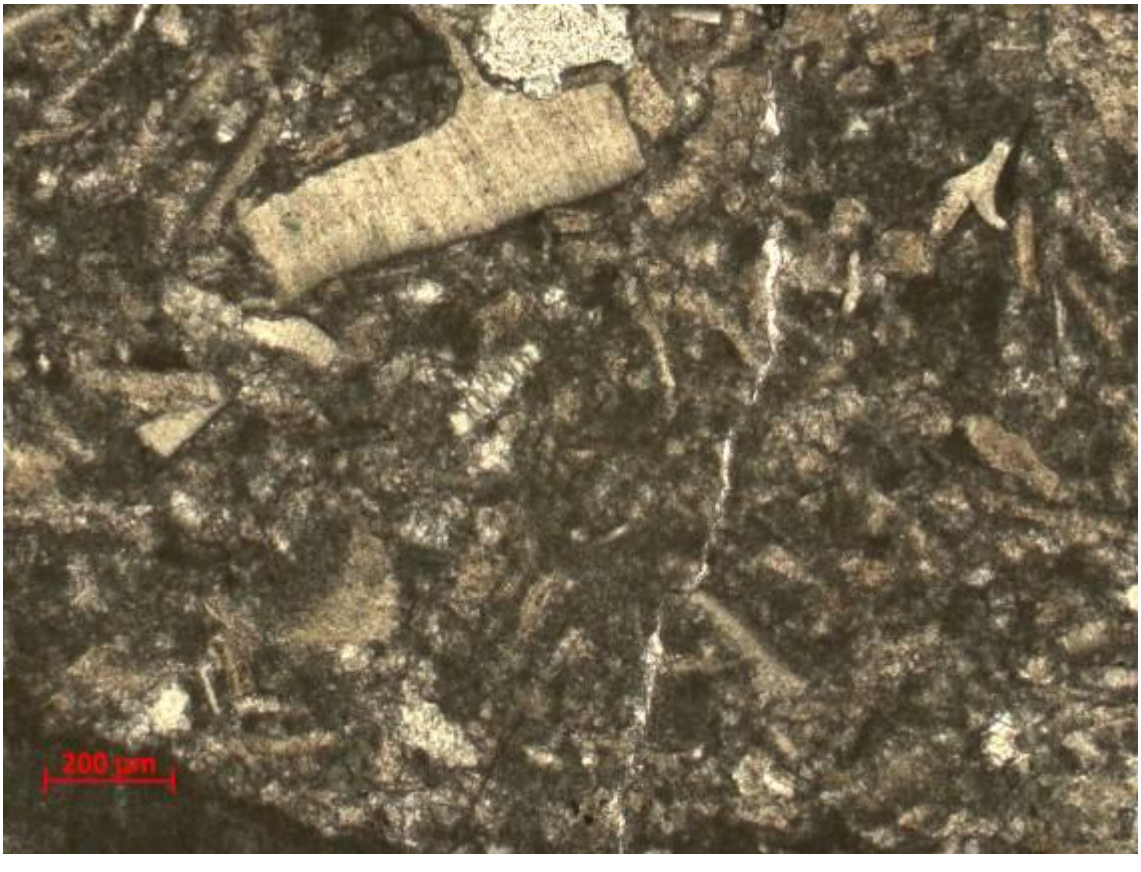

Foto IVB4-9: Partly recrystallised micritic matrix

Location Filipčje Brdo: SAMPLE FB-1

Texture

Sample exhibit relatively homogeneous texture of the medium-grained packstone (photo IVB5-1), where only in one part of the sample the small lens of finer-grained packstone (photo IVB5-2) occur and is oriented parallel to the bedding. In coarse-grained packstone the grain/matrix ratio is around than 50/50 (photo IVB5-1) , while in the loosely-packed packstone the ratio is 40/60 (photo IVB5-1). In the coarse-grained parts the size of the grains ranges from few 10 of µm to few millimeters, on average the grains are around 0,5mm large. In finer-grained packstone the grains are smaller ranging from 40 to 200 µm. In the densely-packed parts the grains are moderately sorted, at places with preserved original shape, while more common sub-angular to sub-rounded. The grains mainly exhibit point, line and concavo-convex contacts. In finer-grained packstone the grains are well sorted, sub-rounded, and exhibit mainly point and line contacts.

In both variations the matrix is micrite that is partly recrystallized into microsparite and in places also sparite..

The sample exhibit no intergranular, moldic shelter and intraparticle porosity. On the other hand the samples exhibit a system of microcracks (discussed in detail in chapter IV-C).

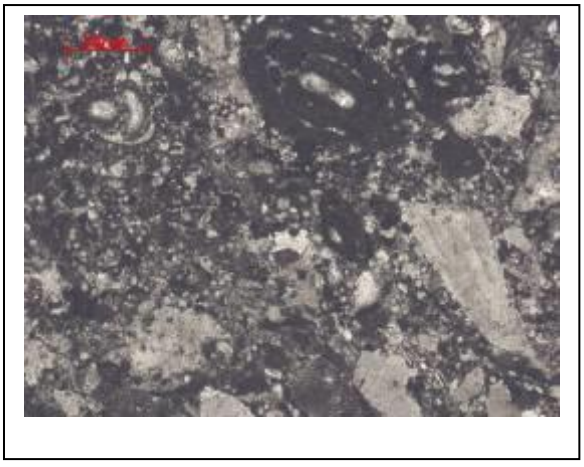

Foto IVB5-1: coarser-graiend packstone with various bioclasts.

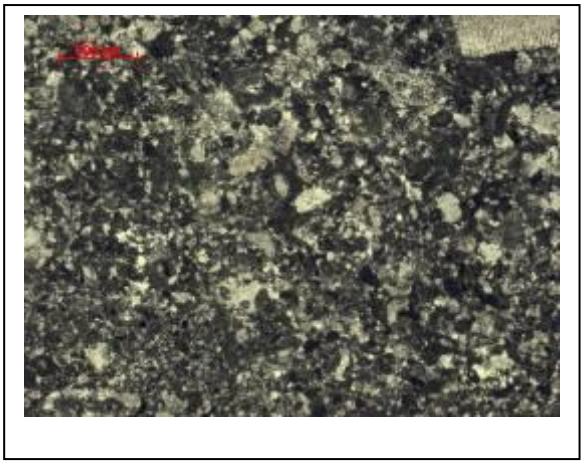

Foto IV5B-2: finer-grained packstone with various bioclasts.

Composition

The grains in the sample constitutes of alochems among which the bioclasts are most common (90%) while intraclasts occur rarely (10%).

Among bioclasts most common are fragments of bivalves (inoceramid and rudist shells?) that represent 70% of grains (photo IVB5-3). They are quite fragmented and range in sizes from 10 µm to few millimeters, on average form 0,5mm large. The fragments are poorly to moderately sorted, usually the internal structure is not preserved due to the recrystallization. They exhibit normal prismatic microstructure composed of the individual calcite prisms that act as a single crystals. Only in rare cases the internal structure is preserved (photo IVB5-3). Other grains are represented by a benthic foraminifers (10%) among which the miliolids are most numerous (photo IVB5-4) while other (textulariidae) are rare. The foraminifers are large up to 1mm, they are moderately sorted, non-fragmented and filled with microsparite. Algae fragments represent next 10% of the bioclasts (photo IVB5-5). They are up to 0,6mm large, with preserved original structure. Echinoderm fragments represent 10% of all bioclasts. They are up to 0,5mm large and at places also exhibit older rim of the syntaxial cements (photo IVB5-6).

Intraclasts are small up to 0,5mm large micritic to microsparitic grains.

Matrix

The matrix of the sample is composed of the micrite that is partly recrystallized into microsparite.

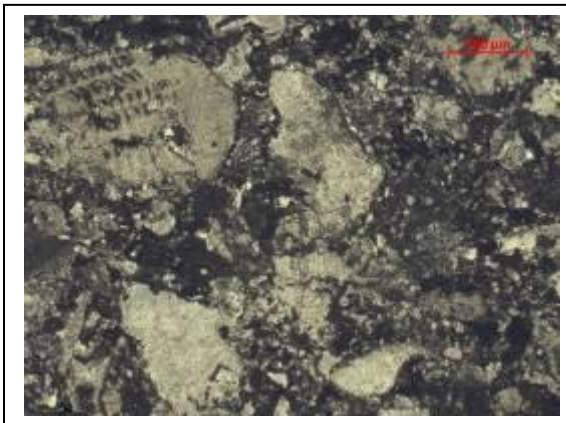

Foto IVB5-3: The bivalve bioclasts with recrystalised and primar strucrure.

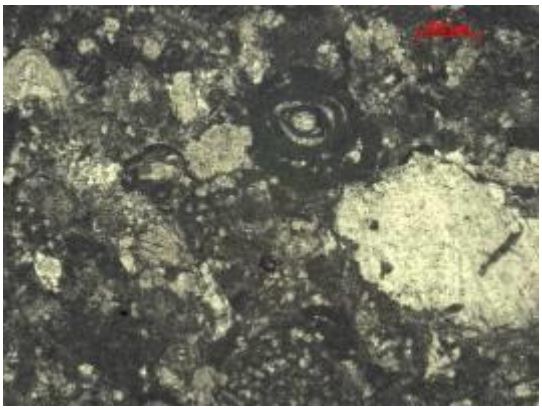

Foto IVB5-4 Pacstone with bioclast of bivales and miliolids.

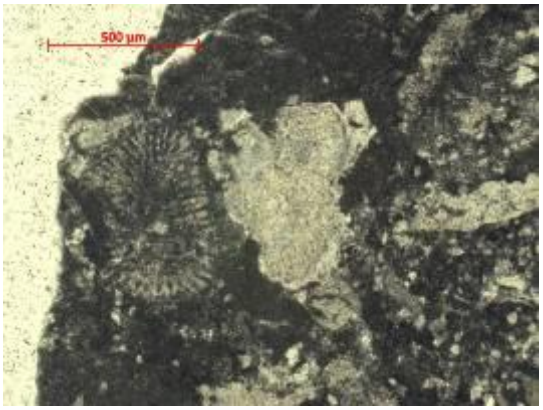

Foto IVB5-5: Alge fragment in the packstone

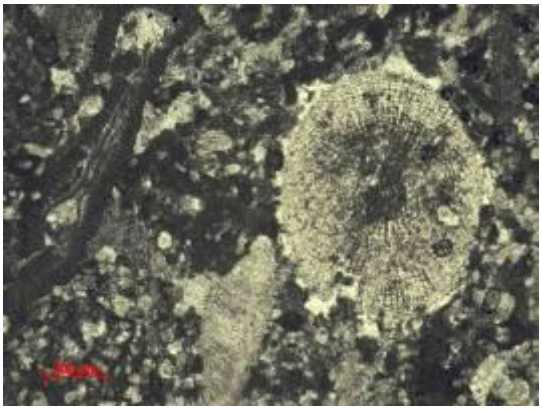

Foto IVB5-6: densely-packed packstone with visible echinoderm fragment.

Location Filipčje Brdo: SAMPLE FB-2

Texture

The texture of the sample is relatively homogeneous texture of the medium-grained packstone (photo IVB6-1). The grain/matrix ratio is around than 50/50 (photo IVB6-1).The size of the grains ranges from few 10 of µm to few millimeters, on average the grains are around 0,5mm large. Only few clasts are bigger can reach up to 0,7mm. The grains are moderately sorted and quite fragmented, thus exhibiting sub-angular to sub-rounded shapes (photo IVB6-2).. The grain contacts are mainly point, line and concavo-convex contacts.

The matrix is micrite that is partly recrystallized into microsparite

The sample exhibit no intergranular, moldic shelter and intraparticle porosity.

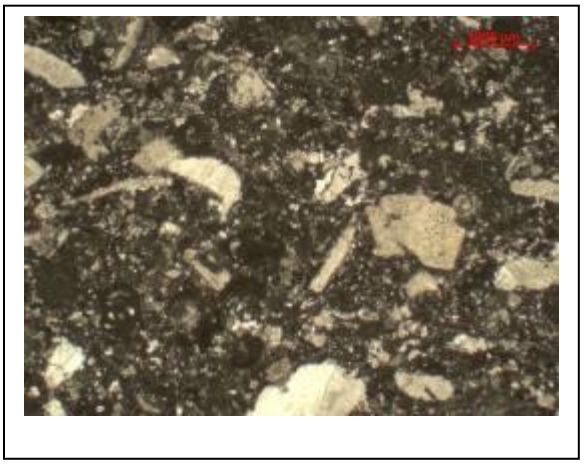

Foto IVB6-1: homogenous pacsktone with bioclasts

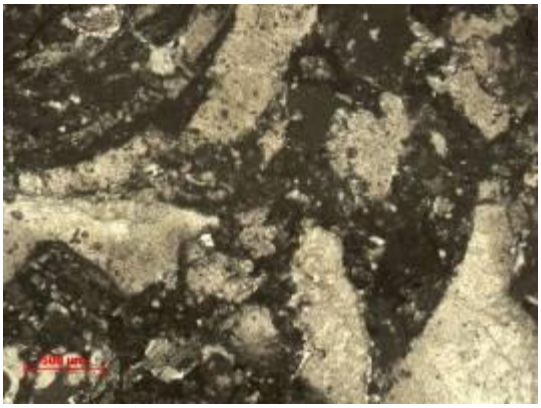

Foto IVB6-2: subangular bioclasts in homogeneous packstone.

Composition

The grains in the sample constitutes of alochems among which the bioclasts are most common (20%) while intraclasts occur more rarely (20%).

Among bioclasts most common are fragments of bivalves (inoceramid and rudist shells?) that represent 70% of grains (photo IVB6-3). They are quite fragmented and range in sizes from 10 µm to few millimeters, on average form 0,5mm large. The fragments are poorly to moderately sorted, usually the internal structure is not preserved due to the recrystallization. Almost all the grains have corroded or bored grain surfaces (photo IVB6-4). Other grains are represented by a benthic foraminifers (10%) among which the miliolids are most numerous (photo IVB6-5) while other

(textulariidae) are rare. The foraminifers are large up to 1mm, they are moderately sorted, non-fragmented and filled with microsparite. Echinoderm fragments represent next 10% of the bioclasts (photo IVB5-6). They are up to 0,5mm large and at places also exhibit older rim of the syntaxial cements however they are usually strongly bored and corroded. Algal fragments are up to 0,6mm large, with preserved original structure and represent 10% of all bioclasts (photo IVB6-7).

Intraclasts constitute 20% of all grains. They are up to 0,5mm large micritic to microsparitic grains. Usually they are elongated and flattened approximately parallel to the bedding (photo IVB6-8).

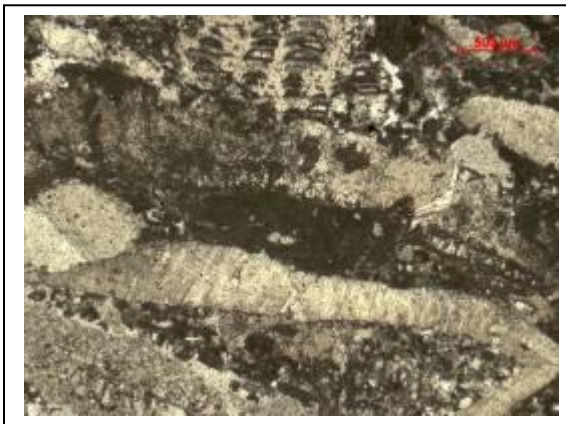

Foto IVB-3: The bivalve bioclasts within the packstone

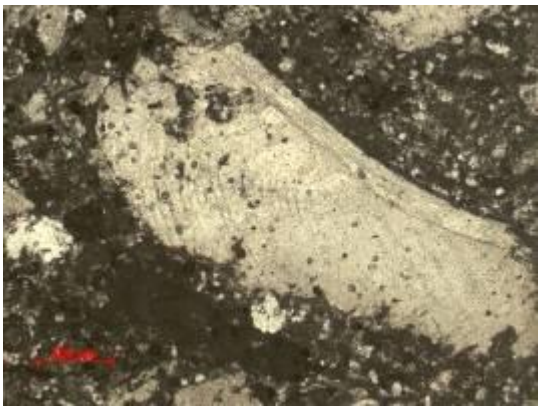

Foto IVB-4 Bored and corrode fragment of the bivalve.

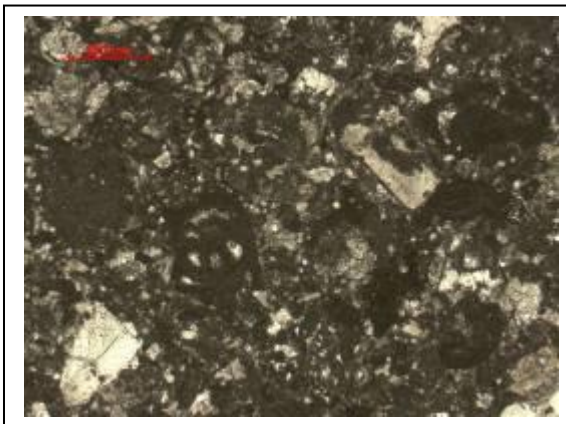

Foto IVB-5: Pacstone with bioclasts of miliolids and bivales.

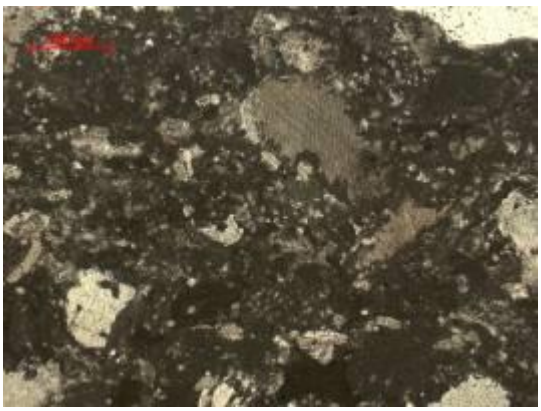

Foto IVB-6: : Pacstone with highly corroded and bored clasts ofechinoederm.

Foto IVB-7: packstone with bivalve and algal fragments.

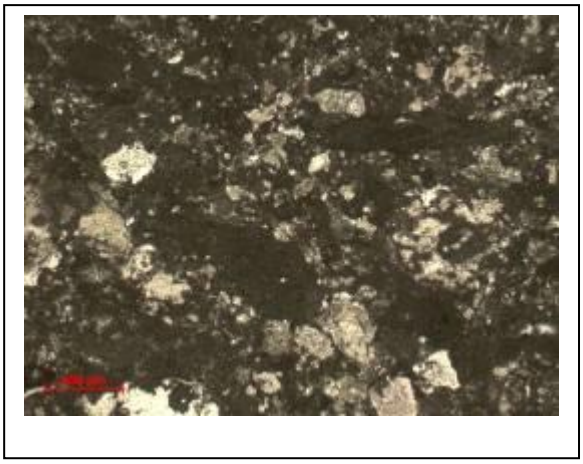

Foto IVB-8: intraclasts within packstone.

Matrix

The matrix of the sample is composed of the micrite that is partly recrystallized into microsparite (photo IVB6-9).

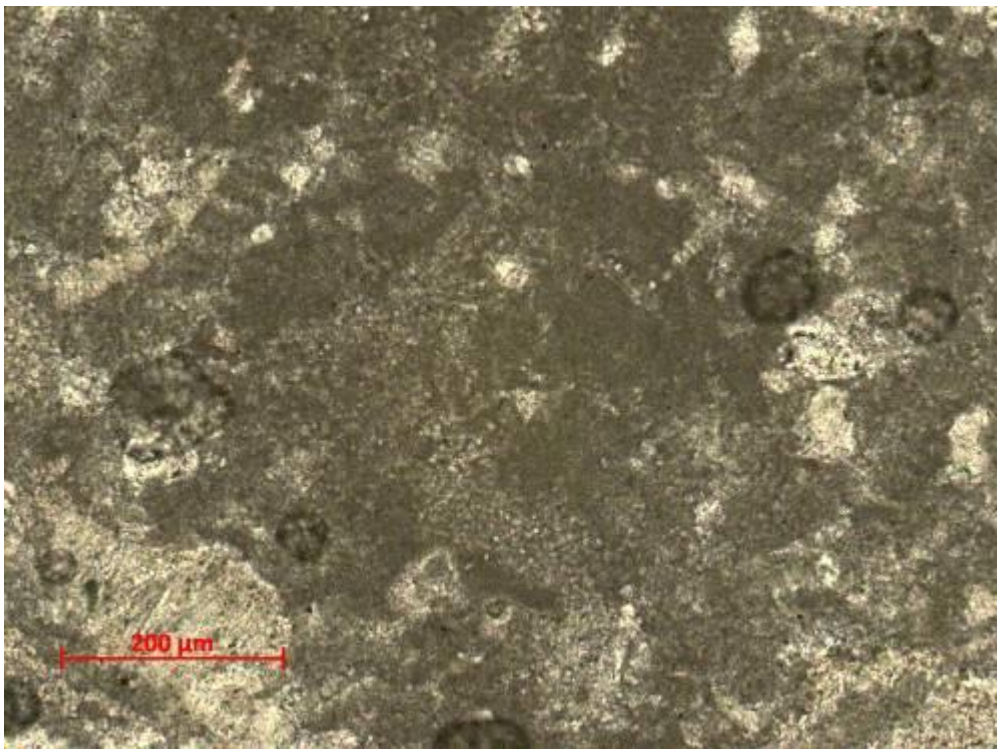

Foto IVB6-9: micritic to microsparitic matrix.

Location Filipčje Brdo: SAMPLE FB-3

Texture

The sample has homogeneous texture of coarse-grained packstone (photo IVB7-1). The grain/matrix ratio is around than 60/40.The size of the grains ranges from 50 of µm to almost 1cm, on average the grains are around 0,5mm to few mm large. The grains are moderately to poorly sorted and quite fragmented, thus exhibiting sub-angular to sub-rounded shapes (photo IVB7-2). The grain contacts are mainly point, line and concavo-convex contacts.

The matrix is micrite that is partly recrystallized into microsparite, however also irregular fields of sparite cement occur within the sample.

The sample exhibit no intergranular, moldic shelter and intraparticle porosity. On the other hand the samples exhibit a system of microcracks (discussed in detail in chapter IV-C).

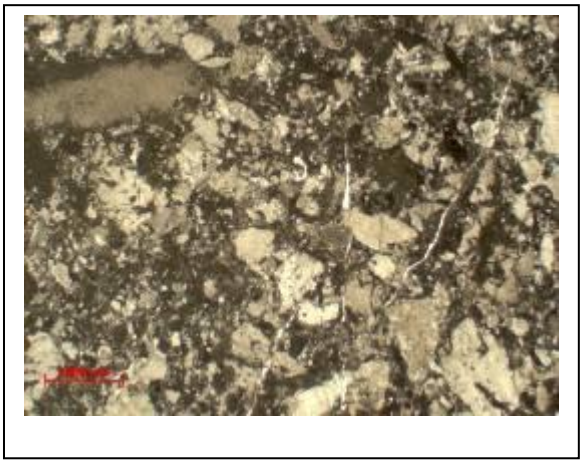

Foto IVB7-1: homogenous packstone with bioclasts

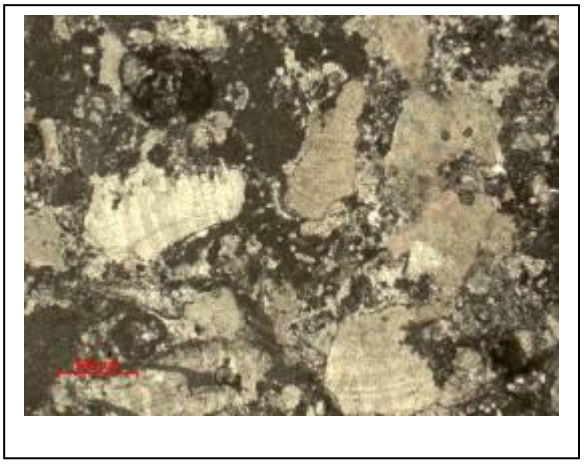

Foto IVB7-2: subangular bioclasts in homogeneous packstone.

Composition

The grains in the sample constitutes of alochems among which the bioclasts are most common (80%) while intraclasts occur more rarely (20%).

Among bioclasts most common are fragments of bivalves (inoceramid and rudist shells?) that represent 60% of bioclasts. They are quite fragmented and range in 50 of µm to almost 1cm, on average the grains are around 0,5mm to few mm large. The fragments are poorly to moderately sorted, usually the internal structure is not preserved due to the recrystallization. Almost all the grains have corroded or bored grain surfaces (photo IVB7-3). 20% of bioclasts are represented by echinoderm fragments. These are also corroded and recrystallized to different degree (photo IVB7-4

and IVB7-5). They can be up to 1cm large. At places the echinoderm fragments show syntaxial overgrowth (IVB7-5). Other grains are represented by a benthic foraminifers (10%) among which the miliolids are most numerous (photo IVB7-6) while other (textulariidae) are rare. The foraminifers are large up to 1mm, they are moderately sorted, non-fragmented and filled with microsparite. Algal fragments are up to 0,6mm large, with preserved original structure and represent 10% of all bioclasts.

Intraclasts constitute 20% of all grains. They are up to 0,5mm large micritic to microsparitic grains (photo IVB7-7).

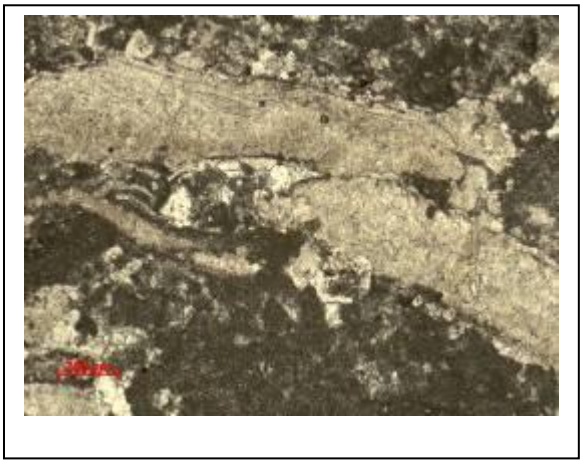

Foto IVB7-3: The bivalve bioclasts within the packstone, clearly exhibiting bored and micritized surfaces.

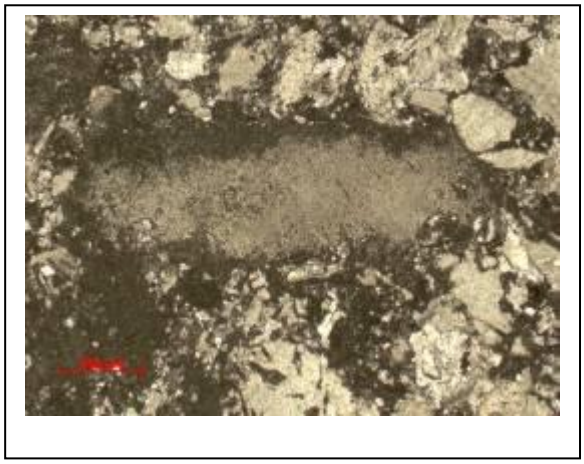

Foto IV7-4 Highly micritized fragment of echinoderm.

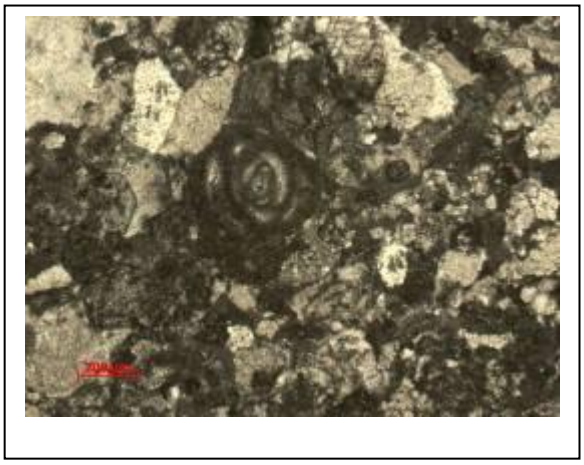

Foto IVB-5: Pacstone with bioclasts of miliolids and bivales.

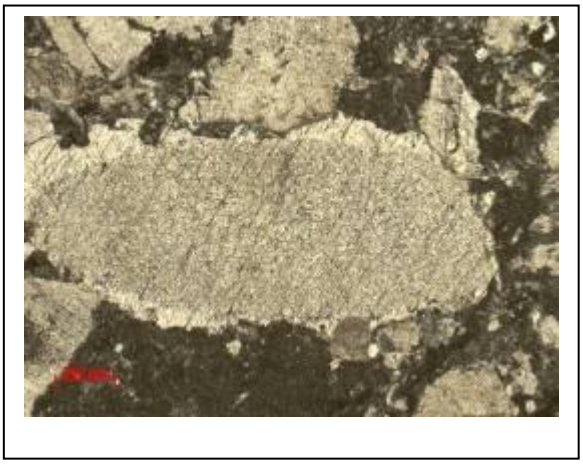

Foto IVB-6: : Pacstone with highly corroded and bored clasts ofechinoederm.

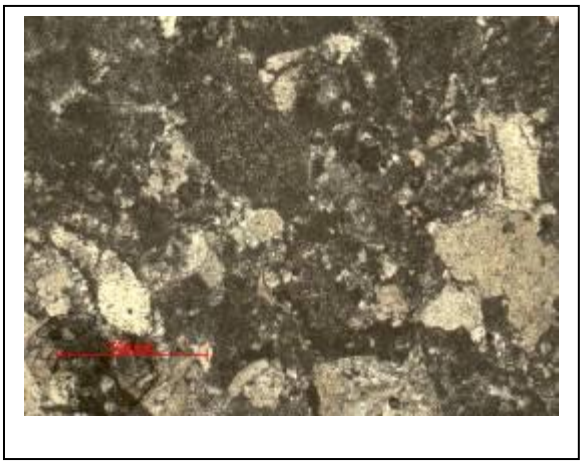

Foto IVB-7: intraclasts within packstone

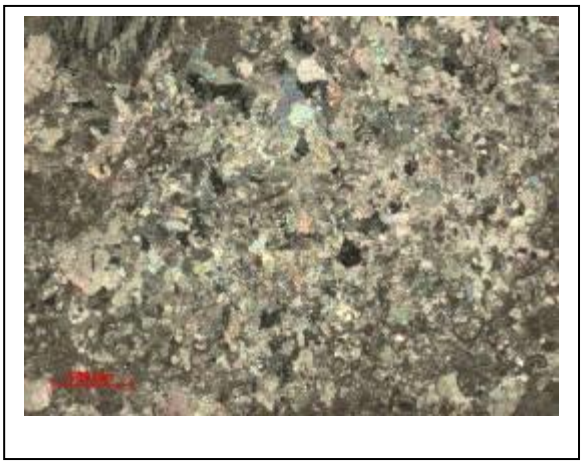

Foto IVB-8: microsparite and sparite matrix.

Matrix

The matrix is micrite that is partly recrystallized into microsparite (photo IVB7-8)., however also irregular fields of sparite cement occur within the sample (photo IVB7-9). Also syntaxial cements around echinoderm fragments are quite frequent (photo IVB7-10).

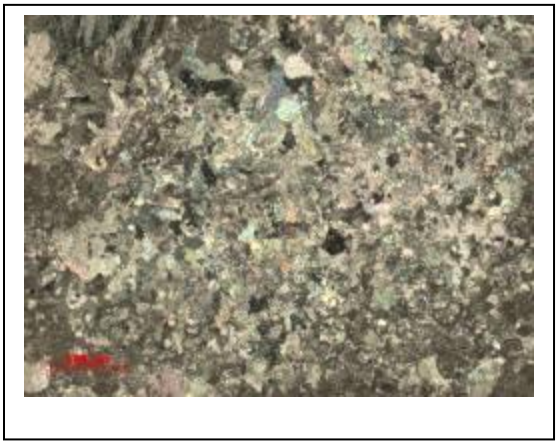

Foto IV7B-9: irregular field of sparite cement

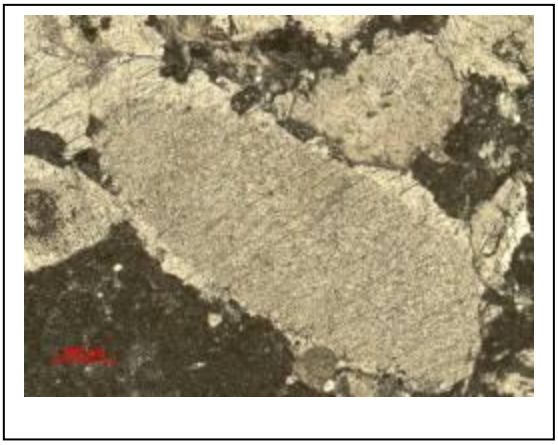

Foto IVB7-107: syntaxial rim around echinoderm fragment.

Location Filipčje Brdo: SAMPLE FB-4

Texture

The sample has homogeneous texture of coarse-grained packstone (photo IVB8-1 and IVB8-2). The grain/matrix ratio is around than 60/40.The size of the grains range from 50 of µm to around 1cm, on average the grains are around 0,5mm to few mm large. The grains are moderately to poorly sorted and quite fragmented, thus exhibiting sub-angular to sub-rounded shapes. The grain contacts are mainly point, line and concavo-convex contacts.

The matrix is micrite that is partly recrystallized into microsparite.

The sample exhibit no intergranular, moldic shelter and intraparticle porosity. On the other hand the samples exhibit a system of microcracks (discussed in detail in chapter IV-C).

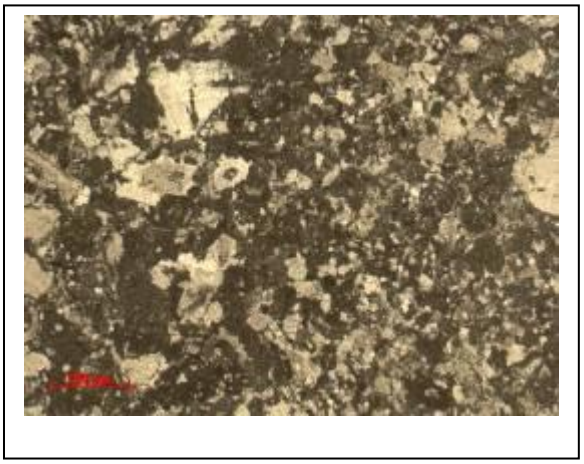

Foto IVB8-1: homogenous pacsktone with bioclasts

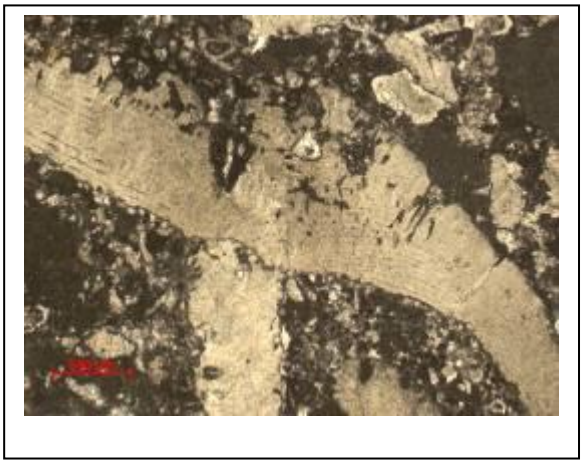

Foto IVB8-2: bored bioclasts in homogeneous packstone.

Composition

The grains in the sample constitutes of alochems among which the bioclasts are most common (80%) while intraclasts occur more rarely (20%).

Fragments of bivalves are most common bioclasts (inoceramid and rudist shells?) and represent 70% of bioclasts. They are fragmented and range in 50 of µm to almost 1cm, on average the grains are around 0,5mm to few mm large. The fragments are poorly to moderately sorted, usually the internal structure is not preserved due to the recrystallization (photo IVB8-3). Almost all the grains have corroded or bored grain surfaces (photo IVB8-2). 10% of bioclasts are represented by echinoderm fragments. These are also corroded and recrystallized to different degree. They can be up to 1cm large. At places the echinoderm fragments show syntaxial overgrowth. Other grains are

represented by a benthic foraminifers (10%) among which the miliolids are most numerous (photo IVB8-4) while other (textulariidae) are rare. The foraminifers are large up to 1mm, they are moderately sorted, non-fragmented and filled with microsparite. Algal fragments are up to 0,6mm large, with preserved original structure and represent 10% of all bioclasts.

Intraclasts constitute 20% of all grains. They are up to 0,5mm large micritic to microsparitic grains, while at places the intraclast grains are mudstones to wackestones with calcispheres (photo IVB8-5).

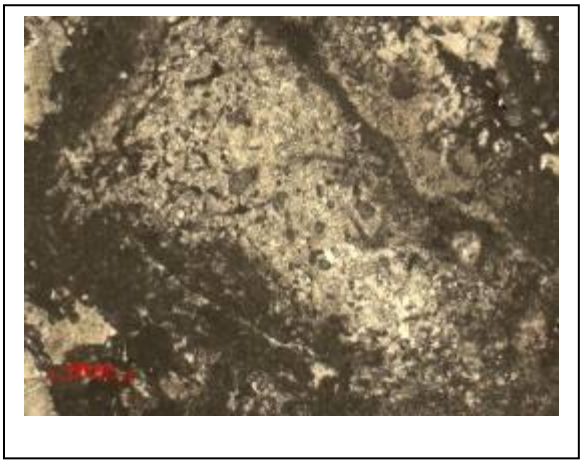

Foto IVB8-3: Strongly recrystalised and bored bivalve bioclasts within the packstone.

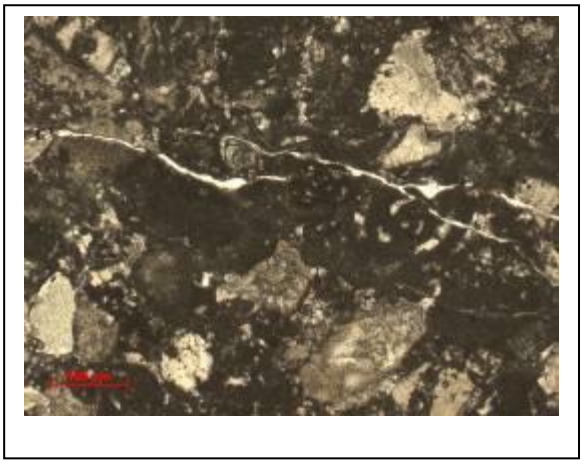

Foto IVB8-4 Pacstone with bioclasts of miliolids and bivales

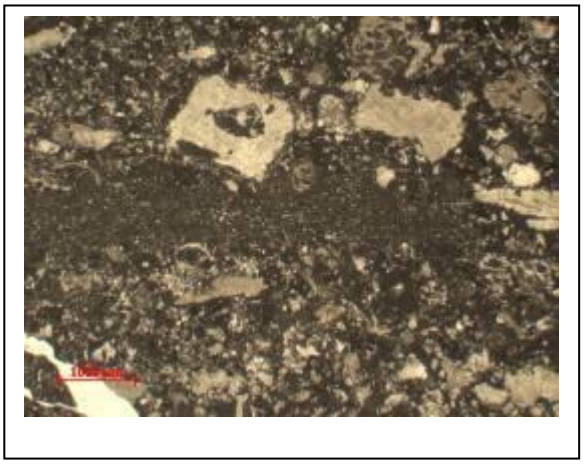

Foto IVB8-5: : intraclasts of wackestone with calcispheres

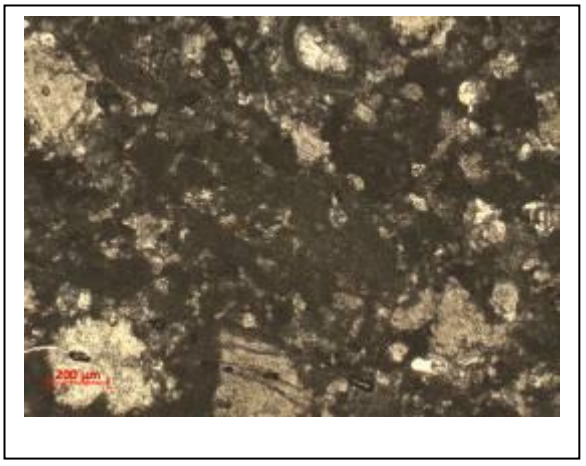

Foto IVB8-6. Microsparitic matrix in packstone.

Matrix

The matrix of the sample is composed of the micrite that is partly recrystallized into microsparite (photo IVB8-6).

IV.C. HOST ROCK MICROTECTONIC

Sample DG -1

The sample is fractured by a system of fissures. Larger individual fissures approximately parallel are spaced between 0,7 to 1,5cm (photo IVC1-1).

These main fissure is continuous across all of the thin section and are up to 150 μm wide (photo IVC1-2). They are well defined individual and relatively straight fracture, and at places forming overstepping architecture (photo IVC1-3). The fissure is opened and at places includes also fragments of the rocks (photo IVC1-4). The fracture walls are smooth and sharp, however at places also week undulating geometry can be found (photo IVC1-5). At wall surface of the fracture there are signs of recrystallization and/or authigenic growth of small sparite cements (photo IVC1-6). The fracture divides the rock into rough to smooth slate domains up to 1cm thick.

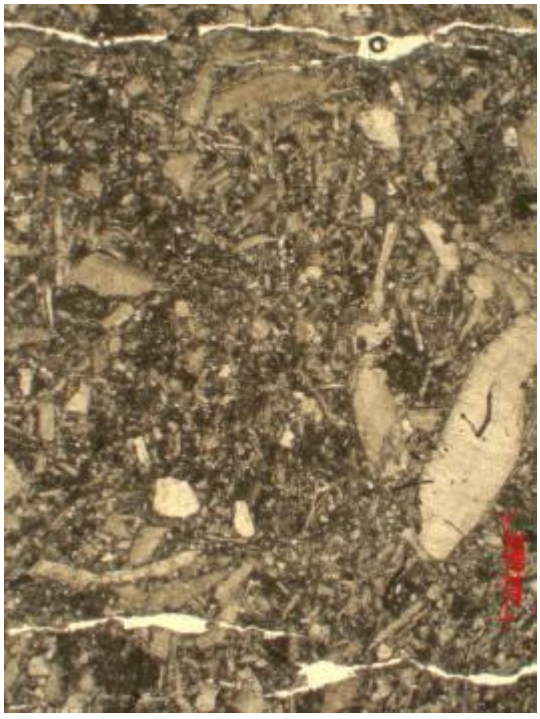

Foto IVC1-1: fissures in grainstones and packstones

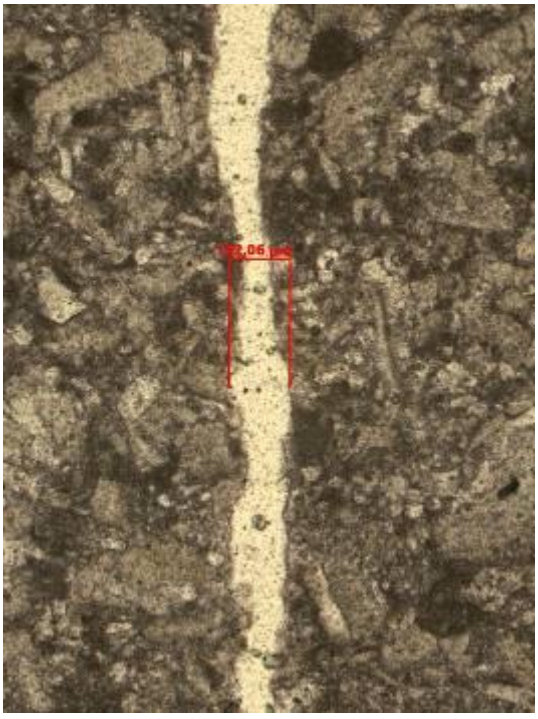

Foto IVC1-2. Main fissure with marked wideness.

Foto IVC1-3: fissures exhibiting overstepping architecture

Foto IVC1-4. Main fissure with still attached rock fragments.

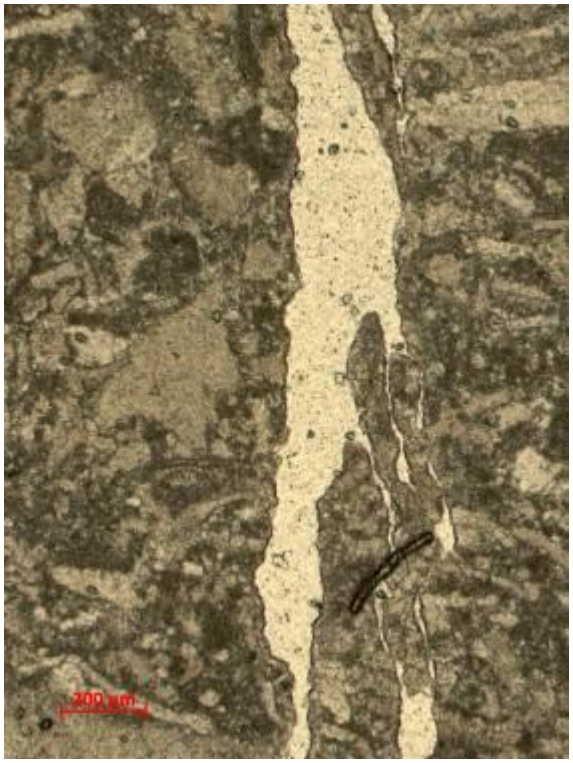

Foto IVC1-5: fissures with straight and smooth walls and sligh undulating surface

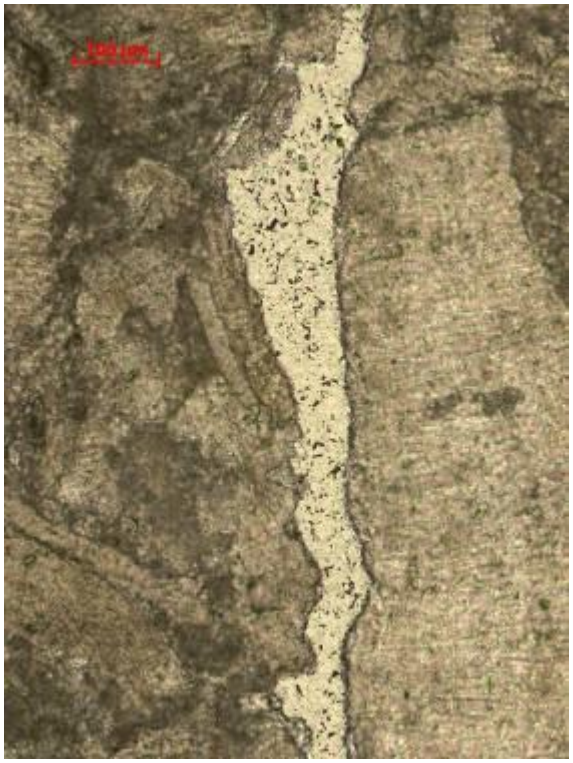

Foto IVC1-6. Small authigenic sparitic-microsparitic grains at the fissure surface.

Sample DG_Z-1

The sample is fractured by a system of fissures. Larger individual fissures approximately parallel are spaced between 0,7 to 1,5cm (photo IVC2-1).

The main fissure can be followed across all of the thin section however at places they are almost closed and present only as a deformed grain to grain contacts (photo IVC2-2). They are up to 130 µm wide (photo IVC2-3). They are well defined individual and relatively straight fracture, and at places forming overstepping architecture (photo IVC2-4). The fracture walls are relatively rough and sharp, however at places also week undulating geometry can be found (photo IVC2-5). At wall surface of the fracture there are no signs of recrystallization and/or authigenic growth of small sparite cements (photo IVC2-6). The fracture divides the rock into rough to smooth slate domains up to 1cm thick.

Foto IVC2-1: fissures in grainstone .

Foto IVC2-2: fissures in grainstone. Visible different deformation, from ope fissure to modified grain to grain contacts.

Foto IVC2-3: fissures in grainstone with marked wideness

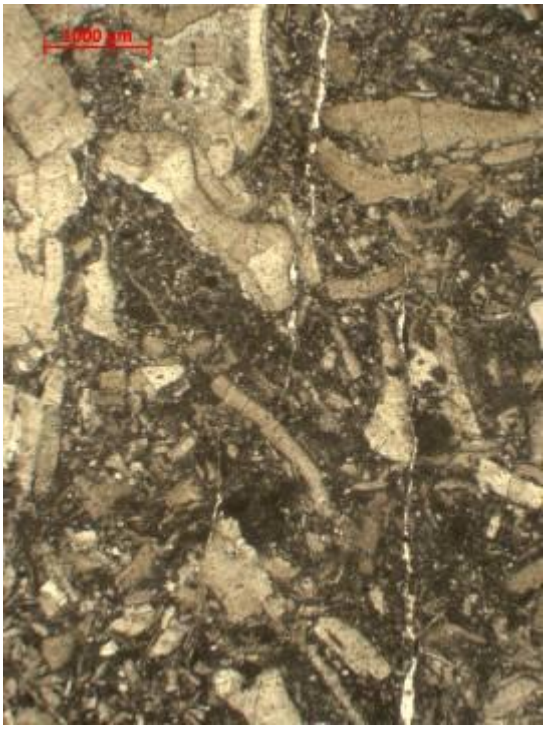

Foto IVC2-4. Fissures exhibiting overstepping architecture.

Foto IVC2-5: Rough and stright walls with sligh undulation.

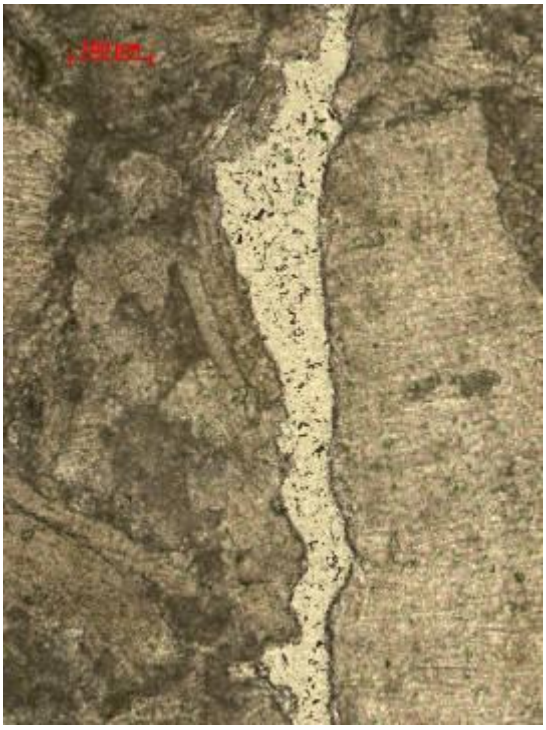

Foto IVC2-6. Rough and stright walls of the fissure.

Sample DG_Z-2

The sample is fractured by a system of weak fissures. Individual fissures approximately parallel are spaced up to 0,7cm (photo IVC3-1).

The main fissure can not be followed across all of the thin section. They terminate at larger grains (photo IVC3-2) or gradually disappear within the matrix (photo IVC3-3). They are up to 100 µm wide (photo IVC3-4). They are well defined individual and relatively straight fracture, and at places include rock fragments (photo IVC3-5). The fracture walls are relatively rough and sharp, however at places also week undulating geometry can be found. At wall surface of the fracture there are signs of selective dissolution of matrix in comparison to the grains (photo IVC3-6).

Foto IVC3-1: Fissure in packstone

Foto IVC3-2. Termination of fissure at the larger grain.

Foto IVC3-3: fissure gradually dissapear in the matrix

Foto IVC3-4. Fissure with marked wideness.

Foto IVC3-5: fissures with rock fragment.

Foto IVC3-6. Selective dissolution of matrix in comparison to the grains in the fissure.

Sample FB -1

The sample is fractured by one thin relatively continuous fracture that at places divides, forming anastamosing architecture (photo IVC4-1).

As said the fissure is continuous across all of the thin section and is up to 90 μm large (photo IVC4-2). It is usually well defined individual and relatively straight fracture, but at places branches into few smaller ones forming horse-tail architecture (photo IVC4-1). The fissure is opened and at places includes also fragments of the rocks (photo IVC4-3). The fracture walls are smooth and sharp, however at places also week undulating geometry can be found (photo IVC4-4). Also at the surface there are no sign of recrystallization or authigenic growth of the calcite cements on the fracture walls.

Foto IVC4-1: fissure forming anastamosing architecture.

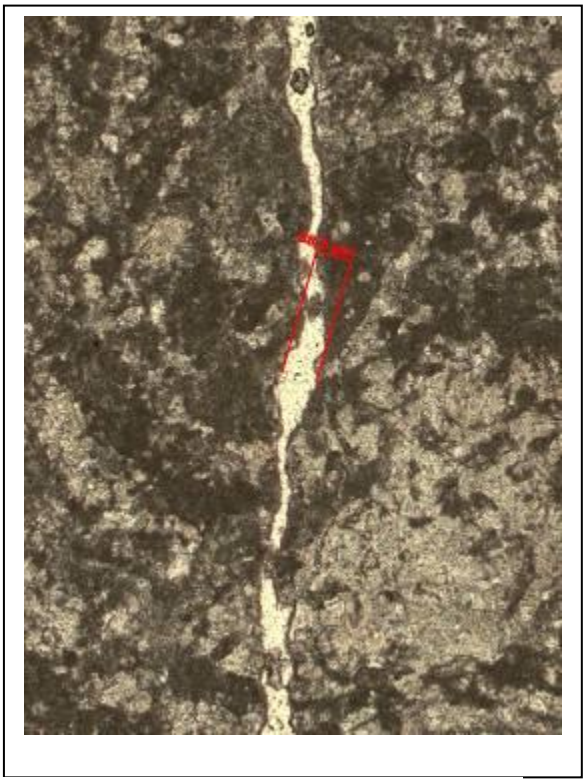

Foto IVC4-2. Fissure with marked wideness.

Foto IVC4-3: fissure containg fragments of the rocks

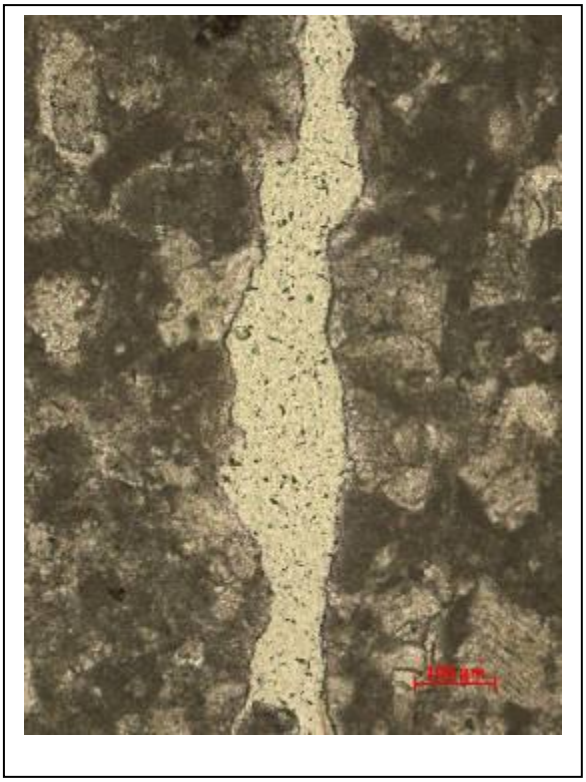

Foto IVC4-4. Fissure with smooth and undulating walls.

Sample FB -3

The sample is fractured by one thin discontinuous fracture that at places forms overstepping architecture (photo IVC5-1).

The fissure is up to 120 μm large (photo IVC5-2). It is usually well defined individual and relatively straight fracture. The fissure is opened and at places includes also fragments of the rocks (photo IVC4-3). The fracture walls are relatively rough and sharp, however at places also week undulating geometry can be found. At wall surface of the fracture there are signs of selective dissolution of matrix in comparison to the grains (photo IVC4-4). Also at the surface there are no sign of recrystallization or authigenic growth of the calcite cements on the fracture walls.

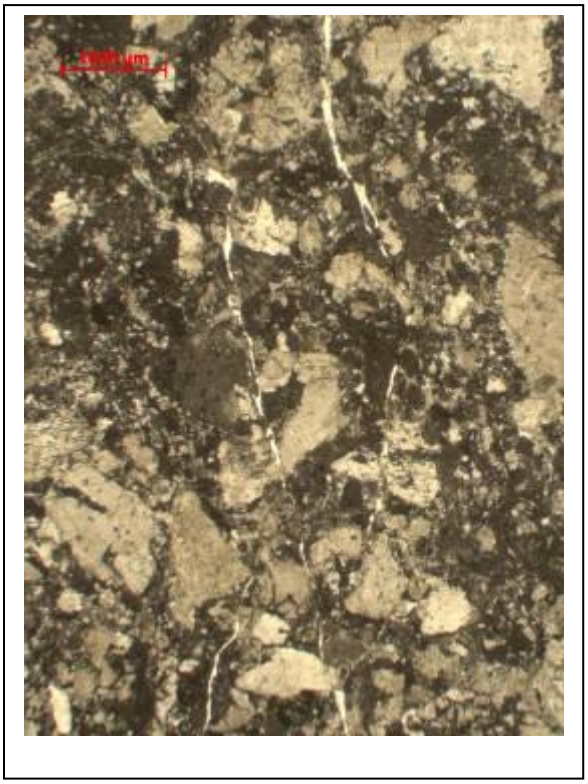

Foto IVC5-1: Fissure with overstepping architecture.

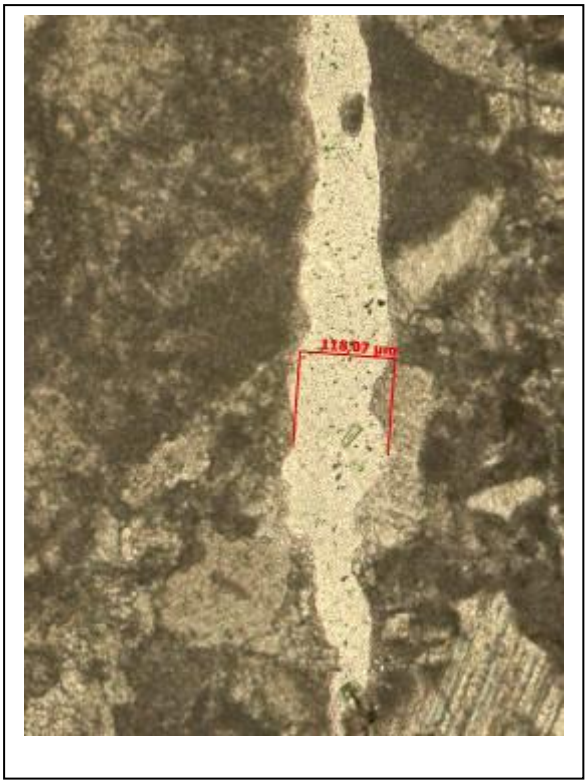

Foto IVC6-2. Fissure with marked wideness.

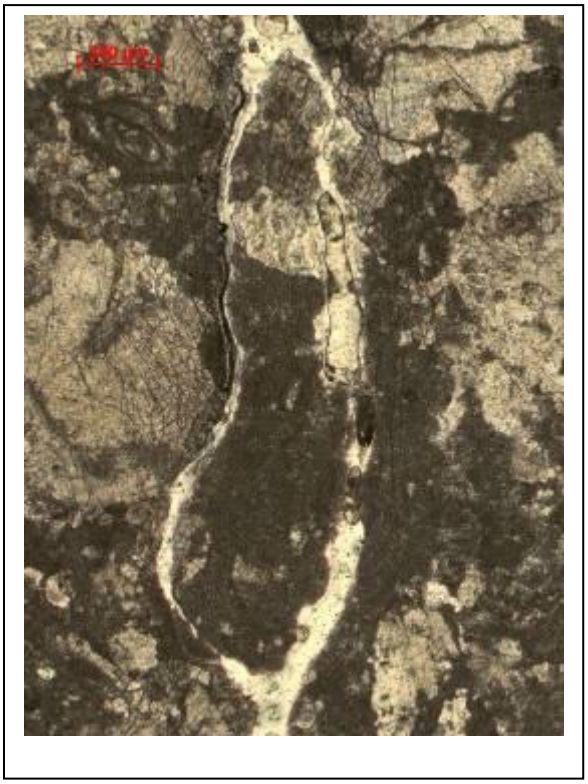

Foto IVC5-3: Fissure with host rock fragments

Foto IVC5-4. Selective dissolution of matrix in comparison to the grains in the fissure..

Sample FB -4

The sample is fractured by two different orientation of fissures that are forming anastamosing spatial relationship (photo IVC6-1).

The main fissure is continuous across all of the thin section and is up to 720 μm large (photo IVC6-2). It is usually well defined individual and relatively straight fracture, but at places branches into few smaller ones forming horse-tail architecture (photo IVC6-6). The fissure is opened and at places includes also fragments of the rocks (photo IVC6-3). The fracture walls are smooth and sharp, however at places also week undulating geometry can be found (photo IVC6-5). Also at the surface there are no sign of recrystallization or authigenic growth of the calcite cements on the fracture walls (photo IVC6-4). The fracture divides the rock into rough to smooth slate domains.

The smaller fissures are up to 30 μm (photo IVC6-7), not continuous across the thin section and are present only at places. The angle between the main fracture and this smaller fractures is form 20 to 30 ^{0}. At places they also show anastamosing architecture (photo IVC6-8). At places it is also visible that the they undergo only slight movement normal to the fracture walls (photo IVC6-9).). The fracture walls are smooth and sharp, however at places also week undulating geometry can be found (photo IVC6-10). The walls of the fracture usually show no sign of recrystallization or authigenic growth of the calcite cements, rarely the small microsparitic spar crystals can be seen at the walls of the fractures (IVC6-12). The fractures are opened, however at places some clay minerals are present (photo IVC6-11, and IVC6-12).

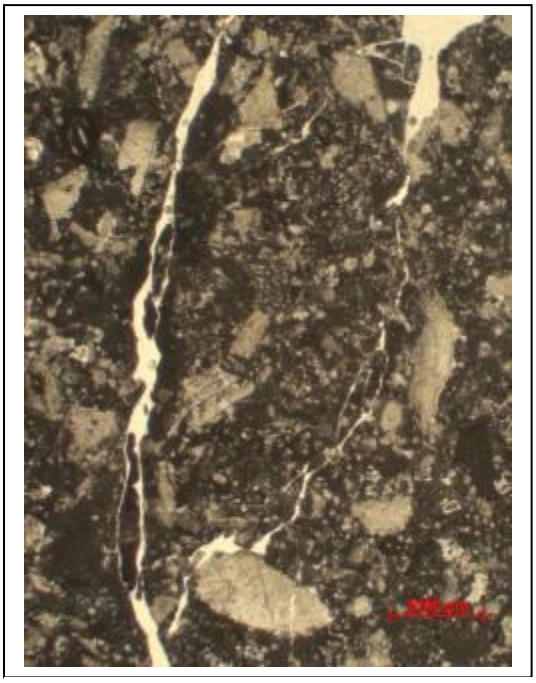

Foto IVC6-1: Fissures of two orientations.

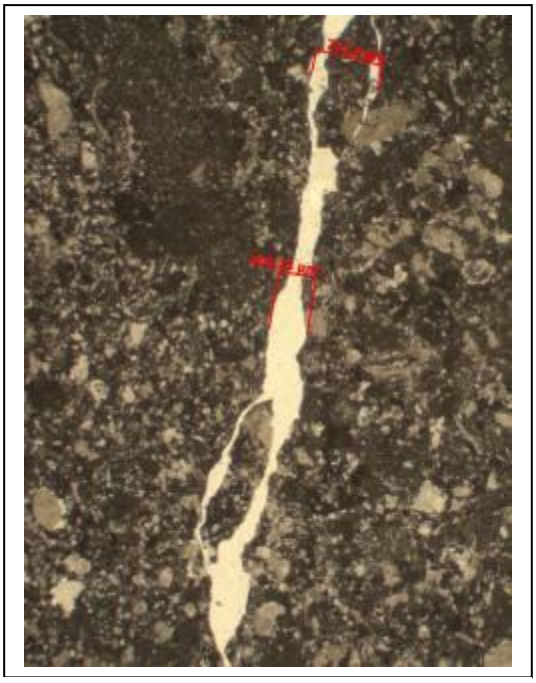

Foto IVC6-2. Fissure with marked width.

Foto IVC6-3: Fissures with fragment of the host rock

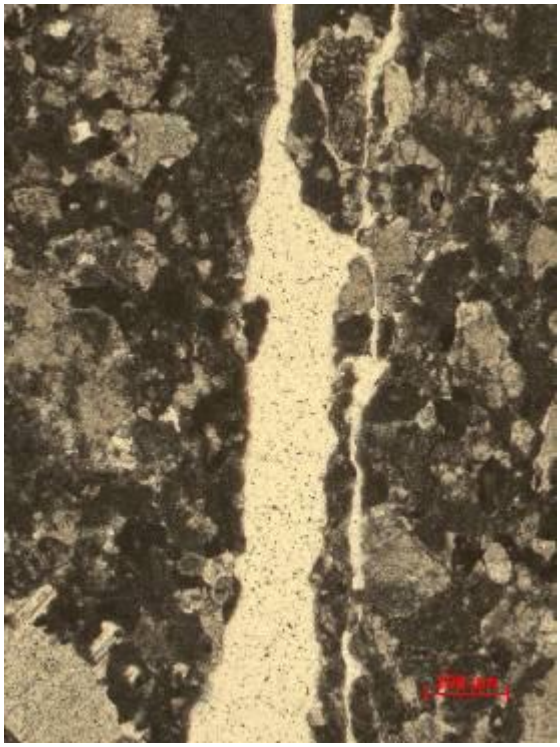

Foto IVC6-4. Smooth walls of the fracture without any sign of recrystallisation.

Foto IVC6-5: Fissure with undulating walls

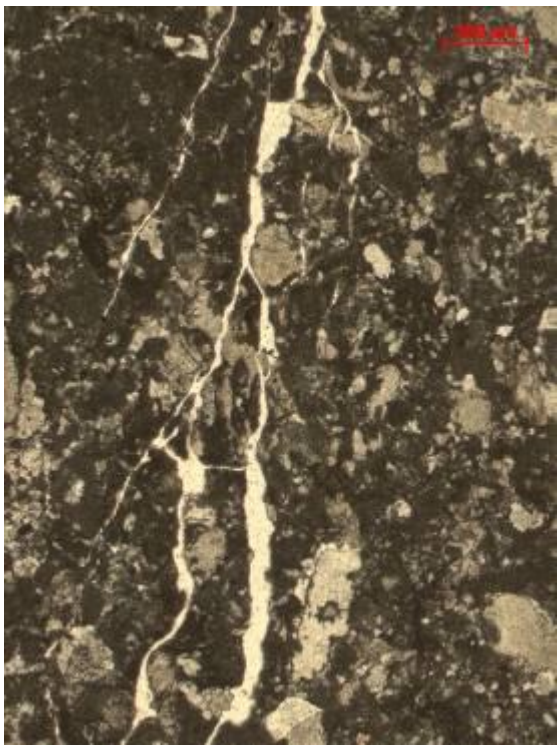

Foto IVC6-6. Branching of the fissure into horse-tail splay.

Foto IVC6-7: Small fissures with marked width

Foto IVC6-8. Anastamosing fissure.

Foto IVC6-9: Fissure with only sligh movement normal to the fissure wall

Foto IVC6-10. Fissure with undulating geometry of the fissure wall.

Foto IVC6-11: Clay minerals in the fissure openings.

Foto IVC6-12. Clay minerals in the fissure openings.

IV.D. SEM ANALYSIS

Location Filipčje Brdo: SAMPLE FB-3

Scanning of platy limestone sample FB-3 revealed very fine grained, micritic structure of calcite. The grains are mostly loosely distributed on the porous surface, partly representing authigenic growth (figure IVD-1a,b) and are mostly xenotopic.

Beside calcite, traces of insoluble residue remained on the top of calcite grains. They have flaky texture (figure IVD-2a,b) and show Si, Al, K, Mg, and Cl composition (figure IVD-2b), which most probably indicate a kind of mix-layered clay mineral. Cl could indicate presence of some evaporate minerals (?). Prevailing peaks are of Ca-carbonate (calcite) from the surrounding of the flakes.

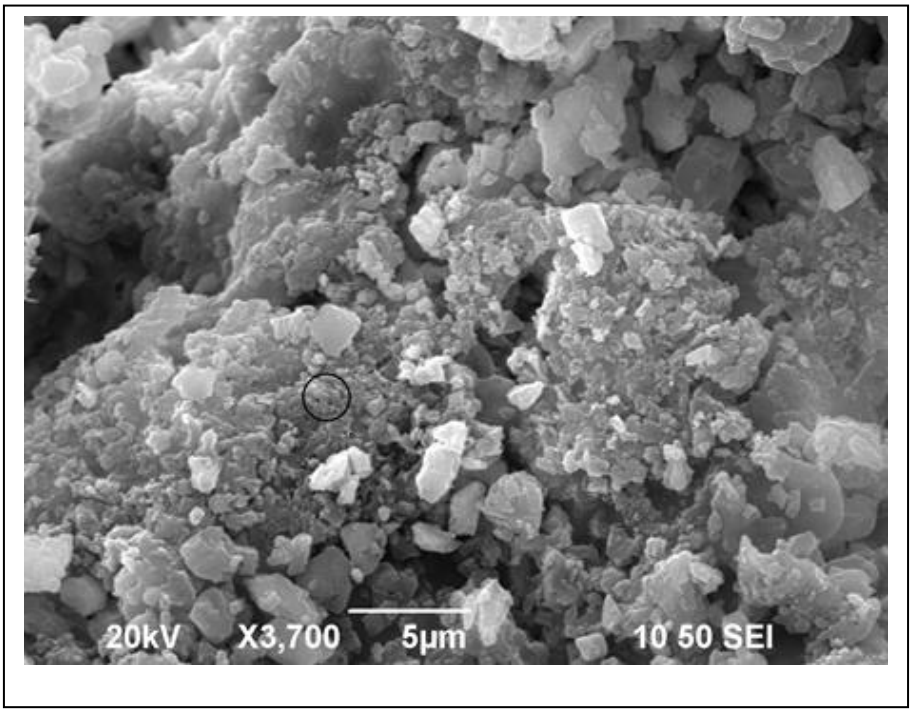

Figure IVD-1a. SE M image of bigger grains of calcite covered by very thin, often platy authigenic calcite. Sample FB-3, Filipčje Brdo.

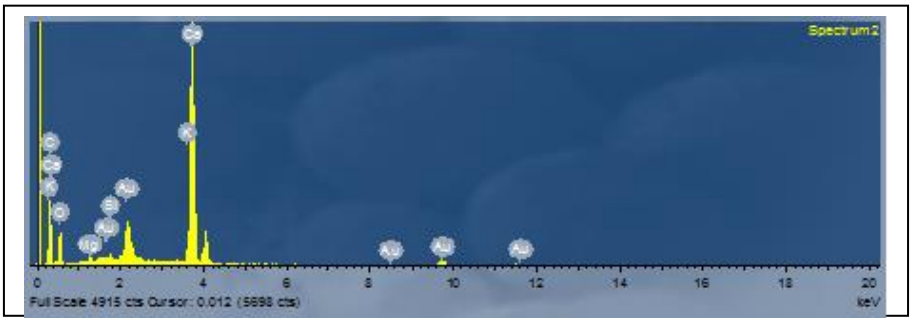

Figure IVD -1b. Chemical composition of calcite with admixtures of clay minerals. Scanned spot marked in Fig. 1a

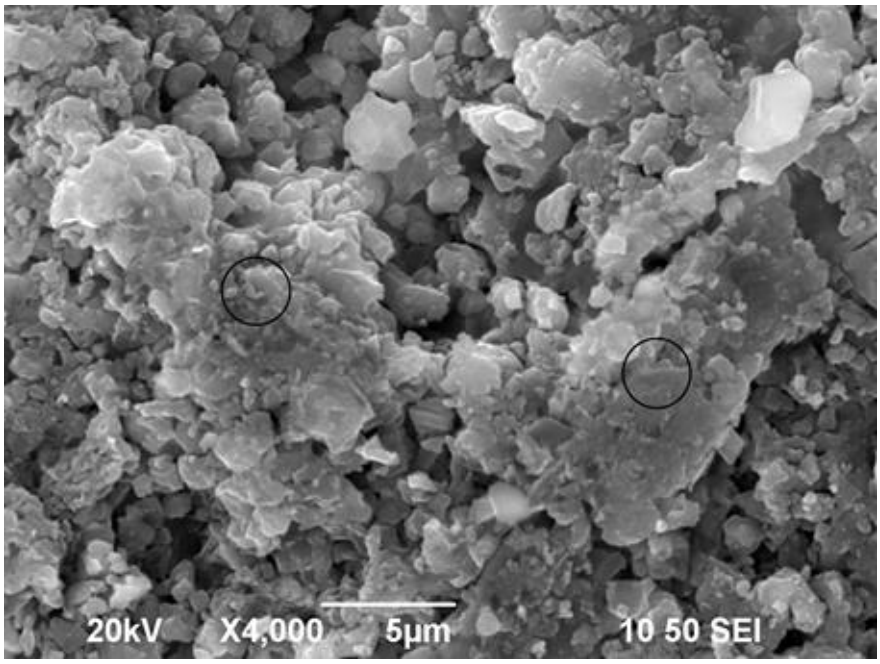

Figure IVD-2a. SE image of thin flakes of clay mineral on top of calcite grains. Composition of marked spots is shown in Fig. 2 b. Sample FB-3, Filipčje Brdo.

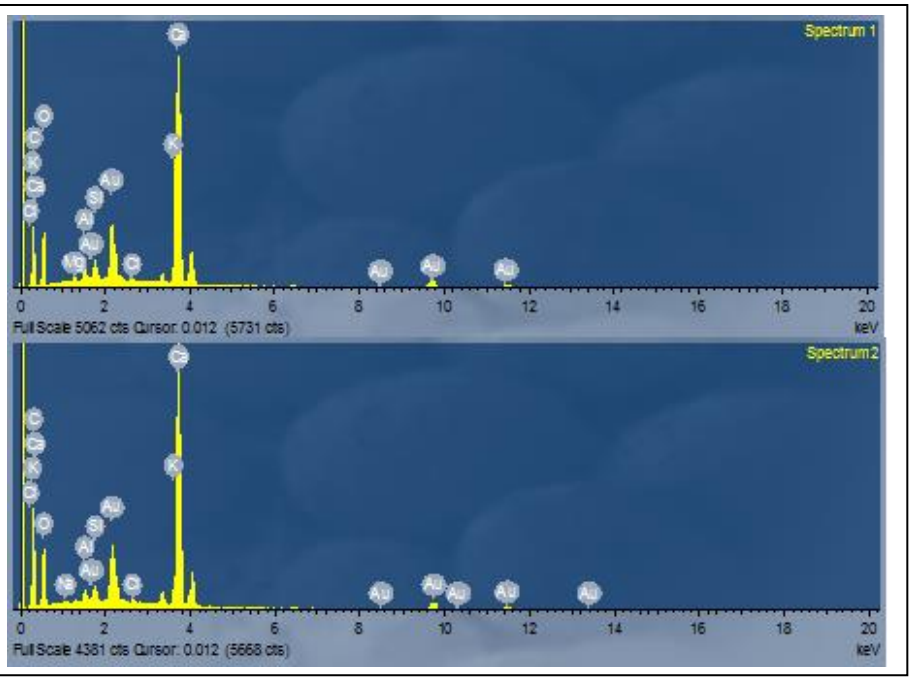

Figure IVD- 2b. Chemical composition of spots marked in Fig. 2a reflects mostly calcite on which clay minerals occur.

Surficial samples of platy limestone contain numerous remains of roots incrusted by calcite (figure IVD- 3) on the bedding planes.

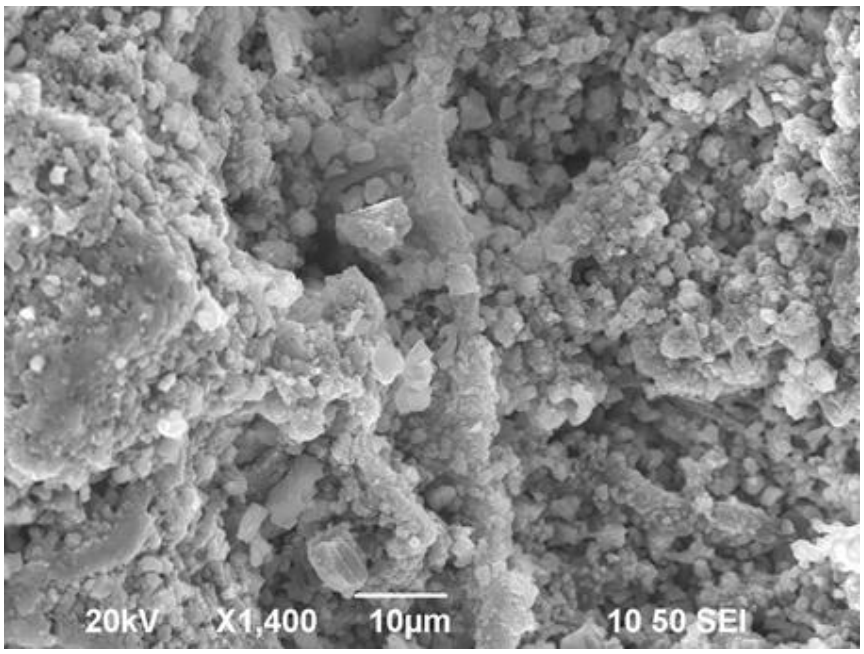

Figure IVD-3. SEM image of hairy root remain (vertical in the centre of the image) incrusted by authigenic calcite. Sample FB-3, Filipčje Brdo.

Location Griža (Tavčar): SAMPLE DG-1

Samples of Debela Griža (Tavčar) limestone quarry are split along cleaved fractures filled with white calcite veins. Two types of surfaces can be seen. Fresh ones, without vein material are micrograined with sparse calcite grains exceeding 0,020 mm in size (figure IVD-4a). Such grain can be seen in the upper center of figure 4. Its chemical composition reveals that probably clay and sulphate(?) minerals grow on its surface (figure IVD- 4b).

Sample surface split along calcite vein has distinct appearance. The surfaces partly consists of calcite crystal clusters (figure IVD- 5a), which grew in an opened space. Locally columnar calcite formed (figure IVD-5b). Grains of calcite are frequently corroded (figure IVD- 5b, 6) indicating dissolution along micro-fractures.

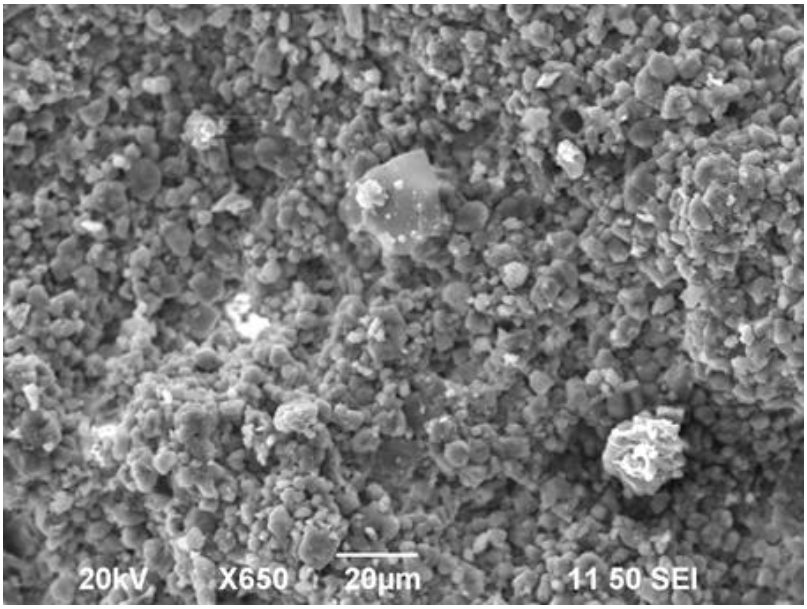

Figure IVD-4a. SE image of fresh cleaved surface of the Debela Griža (Tavčar) limestone quarry. Uniform micrograined texture can be seen. Sample DG-1, Debela Griža (Tavčar) quarry.

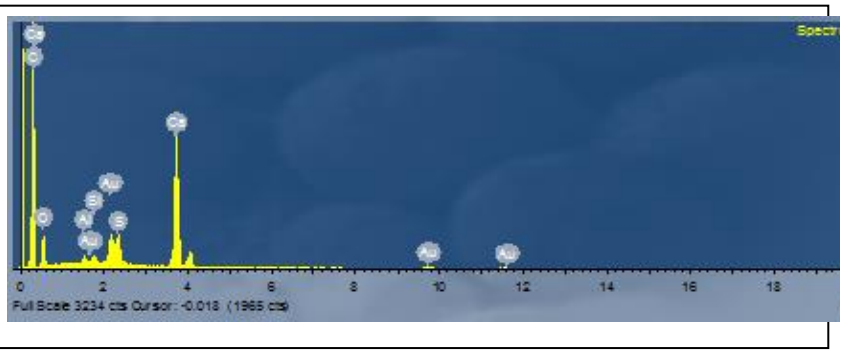

Figure IVD- 4b. Chemical composition of the biggest calcite grain from figure 4a shows that thin grains on its surface could belong to clay minerals and traces of sulphate(?).

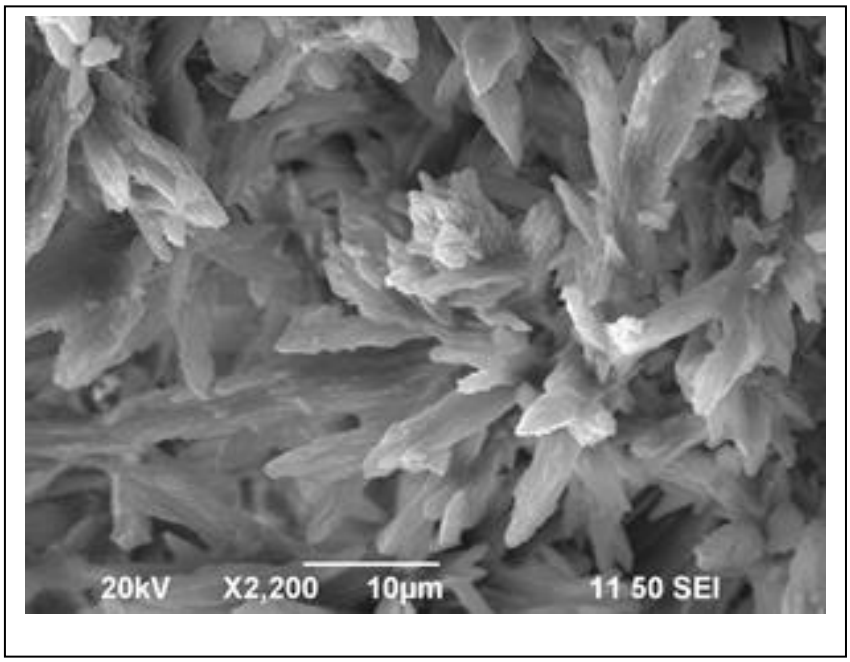

Figure IVD – 5a. SEm image of calcite cluster in a vein of cleaved limestone: formed in a partly opened fracture; sample DG-1

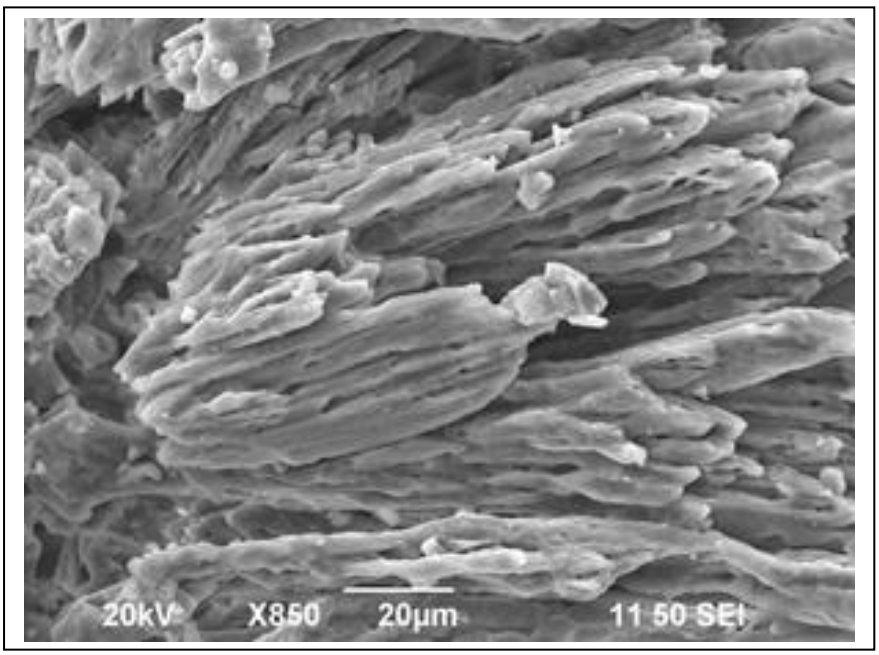

Figure IVD- 5b. SE image of calcite cluster in a vein of cleaved limestone: partly corroded columnar calcite crystals enveloping pores; sample DG-Z-2. Debela Griža (Tavčar) quarry

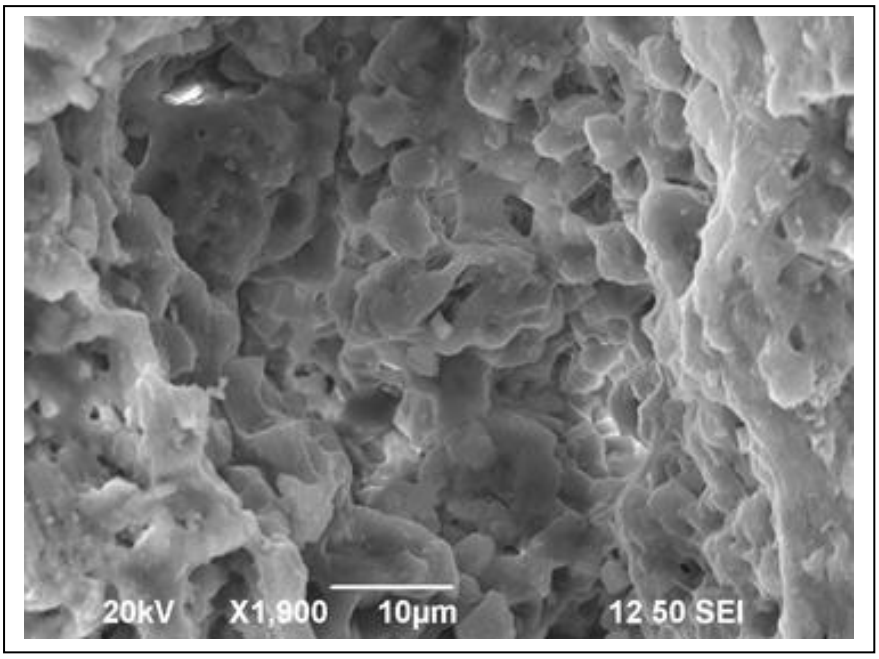

Figure IVD - 6. Corrosion of calcite and formation of pores. SE image; sample DG-Z-2. Debela Griža (Tavčar) quarry.

Ca-carbonate from corroded parts is usually deposited as calcite coatings, but numerous pores remain behind (figure IVD-7).

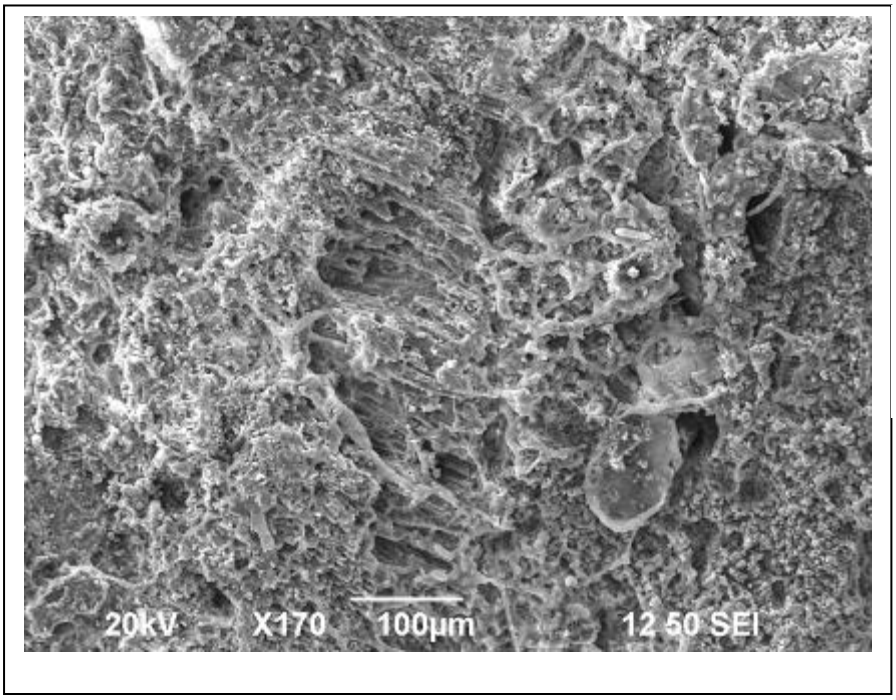

Figure IVD - 7. Corroded surface with frequent pores and thin calcite coatings on the sharp edges. SE image; sample DG-Z-2. Debela Griža (Tavčar) quarry.

In some corroded parts clayey flakes are seen on calcite grains (figure IVD-8), seemingly as on platy limestone of sample FB-3. Their composition is reflected beside calcite in the x-ray spectra of figure 8.

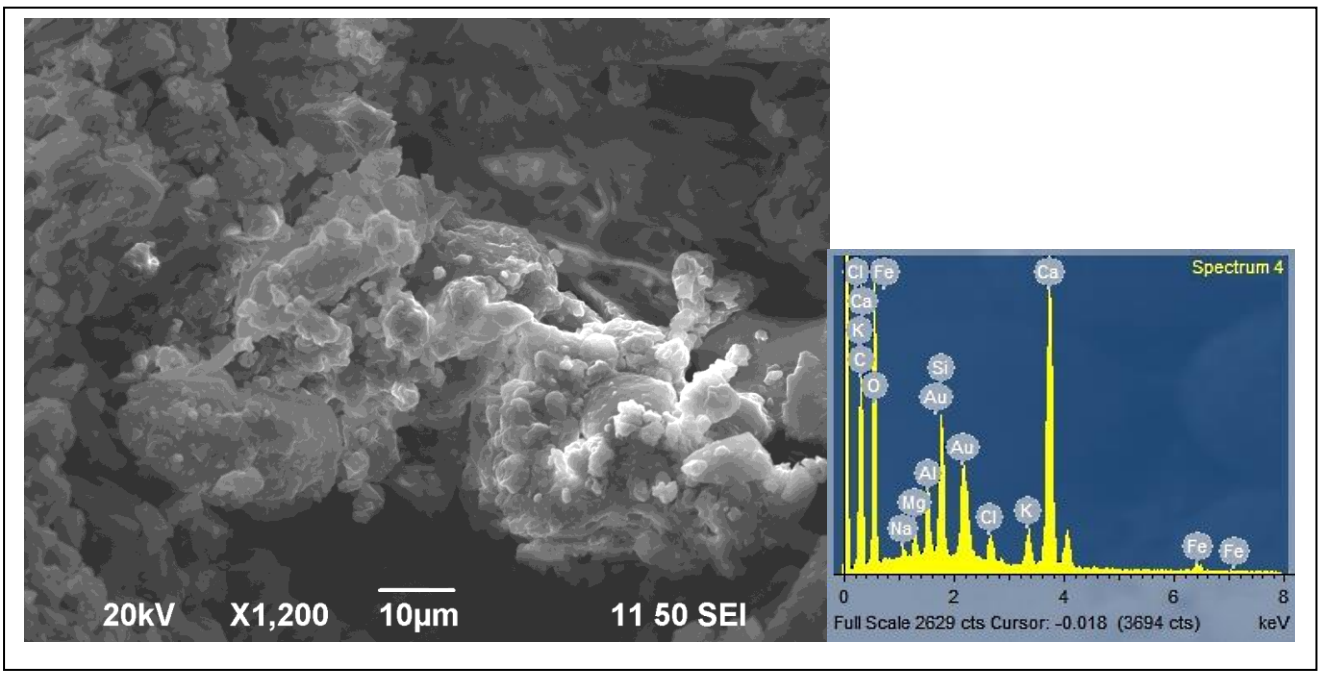

Figure IVD- 8. SE image and x-ray spectra of sparse clay minerals flakes on the surface of the calcite grains. Sample DG-Z-2. Debela Griža (Tavčar) quarry.

V. INTERPRETATION

From the field investigation and detailed sedimentological and microtectonical study (see chapters IV A, IV b, IV C) it is clear that the ''platy'' appearance of the investigated rocks is related to the brittle fracturing of the limestone. The observed plates-slabs are usually perpendicular, or at high angles to the bedding. Even more, the observed joints and fractures in limestones does not appear to follow any of the usual sedimentary or diagenetic suspects (oriented elongated grains, bedding planes, compositional variations within limestone and so on). Additionally the term cleavage is not suitable for this type of the deformation since it requires that rock at the time of deformation preserve some sort of the cohesion, which is not the case here.

The slabs in limestones were produced by formation of closely spaced, approximately parallel fissures-joints (representing fissure system) that divided rocks into thin slabs. We propose a term: **FRACTURED LIMESTONE**, for this type of the limestone slabs to separate them from the ‘’normal‘’ sedimentary slabs.

Origin of fractures and size of the slabs

Joints are simple fractures that do not show any evidence of shear or mineralization and that typically occur perpendicular to the bedding of sedimentary rocks (Hodgson 1961, Price 1966, Hancock 1985, Pollard and Aydin 1988). In a relatively undeformed sedimentary rocks, the density and the height of the joints (opening-mode fractures) are typically controlled by stratigraphy rather that faulting or folding (e.g. Becker and Gross 1996, Hanks et al. 1995, Underwood et al. 2003). Under these conditions, fracture density typically depends on the material properties and bed thickness of the stratigraphic units (Huang and Angelier 1989). Fractures perpendicular to bedding typically initiate within stratigraphic units and terminate at distinct stratigraphic (e.g. Gross et al. 1995). However not all sedimentary contacts terminate fractures (e.g. Corbett et al. 1987, Gross et al. 1995, Hanks et al. 1997, Underwood et a. 2003) so the predictions of fracture networks must consider heterogeneous lithologic control on fracturing. The stratigraphic features that control

fracture initiation and termination in rocks strata comprise mechanical stratigraphy of a sequence (e.g. Gross 1993). A mechanical unit represents one or more stratigraphic units that fractures independently of other units (Fig. 1); mechanical stratigraphic boundaries are generally a subset of sedimentological boundaries (e.g. Corbett et al., 1987; Gross et al., 1995; Hanks et al., 1997; Underwood et al., 2003). Fractures typically span the thickness of the mechanical unit and abut the bounding stratigraphic horizons. Such stratigraphic horizons along which many fractures abut are termed mechanical interfaces (Gross et al., 1995).

Fractures in sedimentary rocks typically initiate from flaws such as fossils, or bugs (Pollard and Aydin, 1988). Flaws concentrate tensile stresses and when these stresses exceed the tensile strength of the rock, the rock breaks along the flaw to become a propagating fracture (e.g. Pollard and Aydin, 1988). The location of fracture initiation therefore depends on the distribution of the largest flaws (Gross, 1993; Renshaw et al., 2003) as well as the tensile strength of the rock.

In our case the fossil dependence in continuation and propagation of the fractures is visible only in one case (sample DG_Z-1) while in all other cases the fractures are composition in depended and cross fossils and even different lithologic varieties of limestones without visible change in the deformation mode.

Since the investigated locations of the quarries lie in the vicinity of the large Divača fault, we believe that the this fault was the driving force for joint initiation, while stratigraphy and sedimentological features (especially bedding) served only as a secondary feature.

Modification of fractures

Almost all of the fractures show (at least in some parts) undulating walls indicating chemical erosion of the host rock. This is not surprisingly since within formations with relatively low matrix-permeability, the architecture of surface fractures, defines potential conduits for fluid flow. For example, thick mechanical units produce tall fractures that provide more direct pathways for fluid migration than thin mechanical units with short, staggered fractures. Short fractures that do not lie in the same plane produce tortuous flow

paths that slow fluid migration and reduce effective bulk permeability (Tsang, 1984).

Additionally the grains of calcite are frequently corroded (figure IVD- 5b, 6) indicating dissolution along micro-fractures. The erosion was not solely related to the chemical weathering, but is also connected to the bioerosion that can act directly and indirectly on the fragmented rocks. Direct effect can be seen as a modification of the fractures by root activity, while indirect effect is related to the formation of soil and humic acids that can chemically erode and modify the existing fractures. The indirect proof for this are rare, but present grains of the clay minerals within the fractures. These minerals were washed into fractures from the up lying soil horizons above the fractures.

VI. REFERENCES

Becker A. & Gross M.R. (1996) Mechanism of joint saturation in mechanically layered rocks: and example from southern Israel. Tectonphysics, 257, 223-237.

Buser S. (1973) Tolmač lista Gorica. Osnovna geološka karta SFRJ 1: 100 000. Zvezni geološki zavod 50 p.

Corbett, K., Friedman, M., Spang, J., 1987. Fracture development and mechanical stratigraphy of Austin Chalk, Texas. The American Association of Petroleum Geologists Bulletin 71, 17– 28.

Dragičević I. & Velić I. (2002) The northheastern margin of the Adriatic Carbonate Platform. Geologica Croatica, 55/2, 185-232.

Gross M.R., Fisher P., Engelder T. & Greenfield R. (1995)factors controling joint spacing in interbedded sedimentary rocks: interpreting numerical models eith field observations frok Monterey Formation, USA. GSA Special publication 92, 215-233.

Gušić I. & Jelaska V. (1993) Upper Cenomanian-Lower Turonian sea-level rise and its consequences on the Adriatic-Dinaric carbonate Platform. Geo. Rundsc., 82/4676-686.

Hancock P.L. (1985) Brittle microtectonics: principle and practuce. Journal of Structural Geology, 7, 437-457.

Hanks C.L., Lorenz J. & Krumhardt A.P. (1997) Lithologic and structural control on natural fracture distribution and behaiour withn the Losburne Greoup, northeastern Brooks range and Northern Slope susurface, Alaska. AAPG Bulletin, 81/10, 1700-1720.

Hodgson R.A, (1961) Classification of stuctures on joint surfaces. Am.J.Sci. 259, 493-502.

Huang Q. & Angelier J. (1989) Fracture spacing and its relation to bed thickness. Geological Magasine, 12/4, 355-362.

Jelaska I., Gušić I., Jurkovšek B., Ogorelec B., Čosović V., Šribar L. & Toman M. (1995) The Upper Cretaceous geodynamic evolution of the Adriatic-Dinaric carbonate platform (s). Geol. Mediterran. 21/3-4, 89-91.

Jurkovšek B., Toman M., Ogorelec B., Šribar L., Šribar Lj., Poljak M. & Drobne K. (1996) Geological map of the southern part of the Trieste-Komen Plateau 1:50 000: Cretaceous and Palogene carbonate rocks. Inštitut za geologijo, geotehniko in geofiziko, 143 p.

Jurkovšek B., Cvetko-Tešović B. & kolar-Jurkovšek T. (2013) Geology of Kras. Geološki zavod Slovenije, 205 p.

Placer L. (1999) Contribution to the macrotectonic subdivision of the border region between Southern Alps and External Dinarids. Geologija 41, 191-221.

Placer L. (2008) Principles of the tectonic subdivision of Slovenia. Geologija 51/2, 205-217.

Poljak M. (2007) Strukturno-tektonska karta Slovenije 1:250 000. Geološki zavod Ljubljana

Poljak M., Živcić M. & Zupančič P. (2000) The seismotectonic characteristics of Slovenia. Pure and Applied Geophysics. 157: 37-55.

Pollard D. & Aydin D. (1988) progress in understanding jointing over the past century. Geol. Soc. Am.Bull., 100, 1181-1204.

Price N.J. (1966) Fault and joint development in brittle and semi-brittle rock. Pergamon Press, 568pp.

Renshaw, C.E., Myse, T.A. & Brown, S.R. (2003) Role of heterogeneity in elastic properties and layer thickness in the jointing of layered sedimentary rocks. Geophysical Research Letters 24

Šribar L. (1995) Evolucija gornjokredne Jadransko-dinarske karbonaten paltforme u jugozapadnoj Sloveniji. Magistarski rad, 89 pp.

Steuber T., Korbar T., Jelaska I. & Gušič I. (2005) Strontium-isotope stratigraphy of Upper Cretaceous platform carbonates of island of Brač (Adriatic Sea, Slovenia). Ann. Nathurhist. Mus. Wien. 97A, 1-19.

Tsang, Y.W., 1984. The effect of tortuosity on fluid flow through a single fracture. Water Resources Research 20, 1209–1215.

Underwood C.A., Cooke M.L., Simo J.A. & Muldon M.A. (2003) Stratigraphic controls on vertical fracture pattern in Silurian Dolomite, northeastern Wisconsin. AAPG Bulletin, 87, 121-142.

Vlahović I., Tišljar J., Fuček L., Oštrić N., Prtoljan B., Velić I. & Matičec D. (2002) The orifgin and importance of the Dolomite-Limestone breccia between the Lover and Upper Cretaceous Deposits of te Adriatic Carboate Platform: An example from Ćićarija Mt. (Istria, Croatia). Geologica Croatica, 55/1, 45-55.

Vlahović I., Tišljar J., Velić I. & Matičec D. (2005) Evolution of Adriatic Carbonate Platform: paleogeography, main events and depositional dynamics. Paleo3., 220, 333-360.

Vrabec M. & Fodor L. (2006) Late Cenozoic Tectonic of Slovenia: Strucrual Styles at the Northeastern Corner of the Adriatic Microplate. In Pinter et al. (eds) The Adria Microplate GPS Geodesy, Tectonics and Hazards. – Nato Science series IV. 151-168.

Vrabec M., Šmuc A., Pleničar M. & Buser S. (2009) Geological evolution of Slovenia – An overwiev. In: Pleničar et la. (eds): Geology of Slovenia. 3-20.